Identification and characterization of 19 predicted Myb-family DNA binding proteins in *Magnaporthe oryzae* concerning growth, conidiation, and pathogenicity

Ya Li[1]*, Xiuxia Zheng[1], Mengtian Pei[1], Mengting Chen[1], Shengnan Zhang[1], Chenyu Liang[1], Luyao Gao[1], Pin Huang[1], Stefan Olsson[1,2]*

[1]State Key Laboratory of Ecological Pest Control for Fujian and Taiwan Crops, College of Plant Protection, Fujian Agriculture and Forestry University, Fuzhou 350002, China

[2]Plant Immunity Center, Haixia Institute of Science and Technology, College of Life Science, Fujian Agriculture and Forestry University, Fuzhou 350002, China

*Correspondence:
Ya Li and Stefan Olsson
liya-81@163.com & Stefan@olssonstefan.com

Running title: Function of Myb family genes in *Magnaporthe oryzae*

Keywords: *Magnaporthe oryzae*; Myb; transcription factors; gene deletion; functional characterization

Author contributions:

Ya Li:
Domain prediction and evolutionary analysis, Myb gene deletions, phenotype tests, protein localization, RT-qPCR, data collection and analysis, figure making, manuscript preparation and writing
Xiuxia zheng:
MoMyb13 gene deletion, MoMyb13 mutant phenotype analysis, MoMyb13 protein localization, RT-qPCR of hydrophobin gene
Mengting Chen, Mengtian Pei, Chenyu Liang, Luyao Gao, Pin Huang:
Myb-gene deletions
Shengnan Zhang:
RT-qPCR of all Myb genes, protein localization of 8 Myb genes
Stefan Olsson:
RT-qPCR extended analysis including PCA and clustering, extended analysis of possible roles of Myb13 and Myb15, manuscript preparation, and writing.

Abstract

Genes encoding for proteins containing the DNA binding Myb domain have been suggested to be important in regulating development and stress response in eukaryotes, including fungi. *Magnaporthe oryzae* (teleomorph *Pyricularia oryzae*) is considered the most destructive pathogen of rice. We screen the *M. oryzae* genome for all genes encoding proteins containing Myb domains since these genes could be essential during pathogenesis. We found 19 genes *Myb1-19*. Only a few have previously been investigated, and only one has proven to be involved in pathogenesis. We tried to delete the other 18 genes and succeeded with all except 6, five of which could be essential. RT-qPCR showed that all 19 genes are expressed during pathogenesis, although at different levels and with different expression profiles. To our surprise, only deletions of the genes encoding proteins MoMyb2, MoMyb13, and MoMyb15 showed growth, conidiation, and infection phenotypes, indicating that they are essential on their own during infection. This lack of phenotypes for the other mutants surprised us, and we extended the analysis to look for expression co-regulation and found 5 co-regulated groups of predicted proteins with Myb-domains. We point to likely compensatory regulations of the other Myb-family genes hiding the effect of many deletions. Further studies of the Myb-family genes are thus of interest since revealing the functions of these genes with a possible effect on pathogenicity since these could be targets for future measures to control *M. oryzae* in rice.

Introduction

Rice blast, caused by *Magnaporthe oryzae* (Teleomorph *Pyricularia oryzae*), is one of the most destructive diseases on rice worldwide. Each year, this disease leads to estimated economic damage of $66 billion, which is enough to feed 60 million people (Pennisi, 2010). The disease initiates from the *M. oryzae* conidia contacting to rice surface, then the conidia germinate and develop a structure called appressoria for host penetration. The mature appressoria accumulate high internal turgor pressure (Howard et al., 1991) and mechanically penetrate rice cells by forming a hyphal peg (Kankanala et al., 2007). Once completing colonization, multiple infection hyphae expand intra- and intercellularly in rice tissue, and the typical blast lesions appear in 3 to 5 days (Sakulkoo et al., 2018). New conidia are produced from lesions and released to start new infection cycles. Besides attacking rice, *M. oryzae* can also infect wheat, barley, finger millet, and foxtail millet (Gladieux et al., 2018). Recently, this fungus caused a wheat blast outbreak in Bangladesh and resulted in huge losses (Islam et al., 2016; Malaker et al., 2016). Given the economic importance, genetic tractability, and genome sequence availability, *M. oryzae* has become a model to study the fungal pathogenesis and interaction with host plants (Dean et al., 2005; Ebbole, 2007). Understanding the transcription-factor-mediated cellular or biological processes of *M. oryzae* is beneficial to develop novel and practical strategies to control the blast disease and ensure global food security.

Based on the similarity of the DNA-binding domain, transcription factors are categorized into up to 61 families, including bZIP, bHLH, C2H2 zinc finger, homeobox, Zn2Cys6, Myb, etc. (Verma et al., 2017). The Myb family is one of the largest and most diverse families characterized by a highly conserved Myb DNA-binding domain (Ambawat et al., 2013; Du et al., 2009; Prouse and Campbell, 2012; Roy, 2016; Verma et al., 2017; L. Wang et al., 2018; X. Wang et al., 2018). The Myb domain generally consists of 1 to 3 imperfect amino acid repeats; each repeat contains 50 to 53 amino acids and spatially constitutes a helix turn helix structure. The name Myb domain was acquired from v-Myb, the oncogenic motif of avian myeloblastosis virus (AMV), where it was first discovered (X. Wang et al., 2018). The Myb family is present in all eukaryotes and could thus have more than 1 billion years of evolutionary history (Eme et al., 2017). The Myb family does not have many members comprising 4 to 5 proteins in animals (Prouse and Campbell, 2012). While in plants, the Myb family has expanded to 100 to 200 members (Prouse and Campbell, 2012). The fungal Myb family size is smaller than in plants but more extensive than in animals with 10 to 50 members (Verma et al., 2017). Animal Myb proteins are reported to regulate cell division and a discrete subset of cellular differentiation events (X. Wang et al., 2018). Plant Myb proteins regulate many metabolic, cellular, and developmental processes especially connected to stress responses (Prouse and Campbell, 2012; Roy, 2016). Fungal DNA binding proteins of the Myb family has been implicated to be essential to withstand stresses (Verma et al., 2017; L. Wang et al., 2018) and consequently to play an essential role in the pathogenicity of plant pathogens (Verma et al., 2017), especially during the necrotrophic phase. In *M. oryzae,* 13 Myb family genes were identified (Verma et al., 2017), and we decided to study the Myb family genes to investigate if any of them singly have roles in the pathogenicity of *M. oryzae* on rice.
First, we searched for the Myb-like domains in *M. oryzae*. We found 19 genes containing Myb DNA binding domains, including *Myb1*, previously proven to be involved in pathogenicity (Dong

et al., 2015). We attempted to delete and complement all the remaining 18 genes and succeeded in deleting 12 genes. Only the deletion of 2 of the 12 genes had a strong effect on pathogenicity when deleted singly. The detailed functions of these genes with effect on pathogenicity should further be studied since these could be targets for future measures to control *M. oryzae* in rice.

Methods

1. Organisms used and media used

Magnaporthe oryzae (B. Couch) anamorph of the teleomorph *Pyricularia oryzae* (Cavara) was used for this research. As background *M. oryzae* strain, we used Ku80 to minimize random integration events (Villalba et al., 2008). The susceptible Indica rice (cv. CO-39) and barley (cv. Golden Promise) used for the fungal pathogenicity test were from the seed bank of our laboratory. The CM (complete medium), MM (minimal medium), and RBM (rice bran medium) used for growing the fungus were prepared as described (Li et al., 2019). The *Escherichia coli* strain DH-5α used for routine bacterial transformations (Li et al., 2015) and maintenance of various plasmid vectors was bought from Solarbio Life Sciences, China.

2. Knockouts, complementations, and verifications

The *Myb* gene deletion vectors were constructed by inserting the 1 kb up-and-down-stream fragments of the target gene's coding region as the flanking regions of the HPH (hygromycin phosphotransferase) gene of the plasmid pBS-HYG (Li et al., 2012). No less than 2 μg of the deletion vector DNA of the target gene was introduced to Ku80 protoplasts, and transformants were selected for hygromycin resistance to perform gene deletion transformations. Southern blotting was conducted to confirm the correct deletion using the digoxigenin (DIG) high prime DNA labeling and detection starter Kit I (11745832910 Roche Germany). The *Myb* gene complementation vectors were constructed by cloning the entire length of the target gene with the native promoter region (about 1.5-kb) to the pCB1532 plasmid. When making the complementation vector, *GFP* was linked to the C-terminal of the target genes to study the sub-cellar localization of Myb proteins. The constructed vector DNA was introduced into the mutation protoplast for the gene complementation assay, and the transformants were screened using 50 μg/ml chlorimuron-ethyl to select successful complementation strains. The detailed fungal protoplast preparation and transformation methods have been described previously (Li et al., 2016). All primers needed for these knockouts and complementations are listed (**Table S1**). The sub-cellar localization of Myb proteins was observed by confocal microscopy (Nikon A1). The excitation wavelength of GFP and RFP were 488 nm and 561 nm, respectively.

3. Colony and growth phenotypes measurements

Vegetative growth was tested by measuring the colony diameter after ten days of growth in 9 cm Petri dishes at 25℃ under 12h-to-12h light and dark periods. Conidia production was evaluated by flooding the 12-day-old colony with double distilled water, filtering out the mycelia by gauze, and counting the conidia using a hemacytometer. The conidiophore induction assay was performed by excising one thin agar block from the fungal colony and then incubating it in a sealed chamber for 24 h with constant light (Li et al., 2010b). Mycelia appressoria were induced by placing a suspension of mycelial fragments on a hydrophobic surface in a humid environment

at 25℃ for 24h. The pathogenicity assay on live rice was performed by spraying 5 ml conidial suspension (5×104 spores/ml) on 15-day-old plants (Li et al., 2014). Post spray, inoculated plants were kept in a sealed chamber with a 90% relative humidity at 25℃ for 24 h. Then, the inoculated plants were removed from the chamber to allow disease symptoms to develop for 4-5 days. The pathogenicity assay on excised barley and rice leaves was performed by cutting a small block from the agar culture of the fungus and placing it on excised leaves for five days in a moist chamber for disease development (Li et al., 2010a). The sexual reproduction was performed by crossing the tested strain with the sexually compatible strain TH3 in OM plates and then incubating at 19℃ for 30 days with continuous light. The perithecia and clavate asci were photographed by a microscope equipped with a camera (OLYMPUS BX51).

4. RT-qPCR

Total RNA was extracted using Eastep®Super Total RNA Extraction Kit (Promega (Beijing) Biotechnology, LS1040) to perform RT-qPCR, and 5 mg of RNA was reverse-transcribed to cDNA using the Evo M-MLV RT kit with gDNA to clean before the qPCR (Accurate Biotechnology (Hunan), AG11705) according to the manufacturer's instructions. The resulting cDNA was then diluted ten times and used as the template for qPCR. The qPCR reactions were performed using an Applied Biosystems 7500 Real-Time PCR System. Each reaction contained 25 ul of SuperRealPreMix Plus SYBR Green (Tiangen Biotechnology, Beijing, FP205-02), one μl of cDNA, and 1.5 μl of each primer solution. The thermal cycling conditions were 15 min at 95 ℃ followed by 40 cycles of 10 s at 95 ℃ and 20 s at 60 ℃. The threshold cycle (Ct) values were obtained by analyzing amplification curves with a normalized reporter threshold of 0.1. The relative expression value was calculated using the 2-ΔΔCT method (Livak and Schmittgen, 2001).

5. PCA analysis and clustering

We used the freeware PAST (Hammer et al., 2001) version 4.08 (released November 2021) for PCA analysis. It is available from the University of Oslo, Natural History Museum https://www.nhm.uio.no/english/research/infrastructure/past/ . The data was handled and entered in MS Excel and then copy-pasted into PAST for analysis. For the PCA, we used correlation of the data for the different genes since they have different average expression levels. The same data was also presented using the clustering function to present the data in a more standard way. In addition, we normalized the expression for each gene against the average expression of the gene during infection to focus the analysis on the expression profiles at increasing HPIs.

Results

1. Myb family domain protein identification in *M. oryzae* and phylogenetic analysis of their relationships

Genes for 19 *Myb* family transcription factors were predicted in *M. oryzae* by Fungal Transcription Factor Database (FTFD, http://ftfd.snu.ac.kr/index.php?a=view). One gene was previously reported as MoMyb1 (Dong et al., 2015), and 9 more recently identified as *MoMyb2-10* (Lee et al., 2021) while we were writing up this work. The other 9 are named *MoMyb11* to *19* in this study (**Fig. 1**). Protein size and domain structure analysis showed that the 19 MoMyb protein sizes vary from the maximum 2305 aa to the minimum 250 aa, and each protein consists of at least 1 Myb domain and up to 3 (**Fig. 1A**). According to amino acid sequence similarities, the 19 M. oryzae Myb domain-containing proteins cluster into four main groups (**Fig. 1B**). To investigate some of the possible biological functions of MoMyb-proteins and especially if some of the Myb proteins, other than MoMyb1 and MoMyb8 (Dong et al., 2015; Lee et al., 2021), are involved in the pathogenesis of rice in *M. oryzae*, 12 Myb gene deletion mutants (*⊿momyb2, 3, 4, 5, 6, 8, 9, 10, 13, 15, 16, and 18*) were generated and confirmed by Southern blot (**Fig S1**). Mutants of 5 other *Myb* genes (*MoMyb7, 11, 12, 17, 19*) could not be obtained, even when screened from more than 200 transformants of each gene, containing the gene fragment that potentially can replace the target gene. *MoMyb7* has been deleted before (Lee et al., 2021); even if we could not achieve a mutation for this one, our lack of mutations indicates that *MoMyb17, 19, 11, and 12* could be essential genes.

2. Only MoMyb2, 13, and 15 are involved in regulating *M. oryzae* growth among the newly found and deleted MoMyb encoding genes,

A growth assay was performed by growing the mutants on three types of media, including complete medium (CM), minimal medium (MM), and rice bran medium (RBM), for ten days (**Fig. 2 and S2**), to analyze whether Myb-proteins have essential roles in *M. oryzae* growth. The colony diameter was tested to evaluate the radial growth rate on the different media. We found 3 MoMyb mutants lacking proteins MoMyb2, 13, and 15 (*⊿momyb2-101, ⊿momyb13-11*, and *⊿momyb15-7*) showed significantly decreased colony size on all three media as compared to the background isolate Ku80 and the corresponding gene complementary strains (*⊿momyb2-101/MoMyb2, ⊿momyb13-11/MoMyb13*, and *⊿momyb15-7/MoMyb15*) (**Fig. 2**). In contrast, the other 9 Myb mutants showed the same colony size as the Ku80 strain (**Fig. S2**), suggesting that MoMyb2, 13, and 15 regulate some aspects of *M. oryzae* growth. The growth inhibition rate of these three mutants on different media was also calculated. The result showed that the mutants show different growth inhibition effects on different media. *⊿momyb13-11* showed the highest inhibition on RBM, followed by MM and CK; *Δmomyb2-101* showed the highest inhibition on CM, followed by MM and RBM; *⊿momyb15-7* showed the highest inhibition on MM, followed by on CM and RBM. The found results are probably because the different nutrients of these media exerted different stress on these 3 Myb mutants. This result also implies that MoMyb2, 13, and 15 possibly regulate the fungal responses to different stresses.

3. Only MoMyb13 and 15 appear to be involved in *M. oryzae* pathogenicity on rice

We tested all the 12 *Myb* gene mutations we had achieved for pathogenicity on rice leaves using

conidia inoculation or inoculation with mycelia on agar blocks. Only *Momyb13* and *15* showed reduced pathogenicity when agar block inoculation was used (**Fig. 3 A-D**), and complementations with their respective gene restored pathogenicity. Conidia inoculation could not be used for these two mutants since no conidia were formed (**Fig. 4**). The lack of pathogenicity does not appear to result from defective appressoria formed from the mycelia (**Fig. 3E**). There were no effects on pathogenicity for the other mutants of the remaining 10 *MoMyb* genes we managed to delete (**Fig. S3**).

4. MoMyb13 and MoMyb15 are involved in conidiation, and MoMyb13 regulates hydrophobins

Since conidia formation is essential for the fungus to spread rice blast disease from plant to plant, conidiation was investigated. A conidia induction assay was performed on CM and RBM media to analyze the function of Myb proteins in *M. oryzae* conidiation. Conidia was absent for both mutants, and their respective complementation completely restored conidiation showing that both MoMyb13 and MoMyb15 are necessary for conidiation, at least on these traditional growth media (**Fig. 4A and B**). Small hydrophobic proteins cover aerial mycelia of many ascomycetes, so-called hydrophobins, making aerial hyphae, including conidiophores, hydrophobic (Bayry et al., 2012; Berger and Sallada, 2019). We had noticed that the *Δmomyb13* had a more wettable mycelium (**Fig. 5A**) and decided to check if any hydrophobins genes were downregulated in *Δmomyb13*. It turned out that *MPG1* was strongly downregulated (**Fig. 5B**). We artificially upregulated *MPG1* in the *Δmomyb13* (**Fig. 5C**), but this did not restore the pathogenicity (**Fig. 5D**), indicating that MoMyb13 regulates more than hydrophobins necessary for successful conidia production and infection of rice.

5. Sensitivity of Momyb13, Momyb2, and Momyb15 mutants to different stresses

A panel of stresses was used to test if the MoMyb mutants affected growth rates on different media. Complete medium (CM) without additions was used as the control medium **(Fig. 6)**. Then the following additions were made to that medium, Sodium Dodecyl Sulfate (SDS); anionic Surfactant affect membrane integrity, Congo Red (CR); affect cell wall integrity, Sodium chloride (NaCl); ionic strength, water potential and eventual sodium toxicity, Sorbitol (SOR): osmotic strength and hydrogen peroxide (H_2O_2); oxidative stress. The MoMyb13 mutant is inhibited by CR and H_2O_2 but stimulated by NaCl and SOR. That can result from a weakened cell wall with less melanization (melanin is an antioxidant) combined with less membrane permeability as compensation for these cell wall weaknesses. Consequently, MoMyb15 and less MoMyb2 mutants are most inhibited by SDS affecting membrane integrity, indicating these two proteins are indeed involved in strengthening the cell wall barrier.

6. The Myb proteins replaced by Myb-GFP localize to the nucleus

All the 18 newly identified Myb-protein-encoding genes were replaced by *GFP*-containing constructs, and the localization of these MoMyb protein GFP-fusions was investigated (**Fig. 7** and **S3**). It was confirmed that all genes we got strong enough GFP signal to visualize through confocal microscopy encode for proteins that localize to the nucleus, as expected for DNA binding proteins containing Myb domains. The three genes that showed changed deletion phenotypes were investigated in more detail in a Histone1-RFP background to mark the nucleus (Zhang et al.,

2019). It became evident that the relatively small green "dots" of the MoMyb2-GFP indicate a localization to the nucleolus, where no other of the MoMybs seems to locate specifically (**Fig. 7** and **S3**).

7. Expression of all identified *MoMyb* genes during infection.

All *MoMyb* genes (1-19) were investigated for expression during different HPI, *in vitro* (MY), and in conidia using RT-qPCR. First, expression values were normalized using the beta-tubulin gene as the housekeeping reference gene. The average expression at all the measured HPI was used for normalization to focus on the *in planta* variation over different HPIs and make easier comparisons of genes. Thus, the analysis focuses on each gene's HPI profiles and makes them comparable. The data was then used to make a PCA analysis of the correlations (**Fig. S5)** shows a PCA bi-plot of the PC1 and PC2 with gene names and variables' (the HPIs, MY, and Con) contribution to the principal components as vectors. In addition, a minimum spanning tree that is nearly equivalent to clustering is also shown (**Fig. S5**). In principle, the same can be visualized in a cluster plot using neighbor-joining clustering (Gower similarity index and final branch as root) (**Fig. 8**) and also in the table with added expression profiles for each gene (**Table S2**) and also compared with blast similarities (**Table S3**). MoMyb2 and 15 appear to have essential roles in the necrotrophic stage and in vitro. On the other hand, MoMyb13 appears to be upregulated and used during the early stage (8h) of plant contact, indicating that it could be a regulator of penetration and establishment in the plant.

MoMyb8 is upregulated both in the early phase and has a peak in the latter and seems to be involved in the light response (Lee et al., 2021). *MoMyb1* has previously been shown to be essential for infection (Dong et al., 2015) and belongs to the regulatory cluster upregulated at 8 HPI. Since we could not find growth or infection phenotypes for more than 3 MoMyb proteins encoded by the newly identified genes, it was expected that some of the *MoMyb* genes are not expressed during plant infection or at all but all were expressed and expressed during different HPIs (**Fig. 8**).

Discussion

The 19 genes predicted to encode Myb domain-containing proteins in *M. oryzae* (MoMyb1-19) by Fungal Transcription Factor Database (FTFD) encodes proteins with very different sizes and content of other domains (**Fig. 1A**). That indicates that they have diverse functions and might not all be traditional transcription factors as often implied since they have a Myb DNA binding domain (Cao et al., 2020; Dong et al., 2015; Du et al., 2009; Dubos et al., 2010; Li et al., 2019; Liu et al., 2015; Roy, 2016; Verma et al., 2017). We found 6 more Myb-domain protein-encoding genes than the 13 *MoMyb* genes identified earlier (Verma et al., 2017) and 9 more than was recently identified (Lee et al., 2021). Interestingly, all 19 MoMyb-protein-encoding genes are expressed at different stages of plant infection (**Fig. 7A**). Thus, it surprised us that the successful deletion of only two of our identified and deleted genes (*Δmomyb13* and *ΔmoMyb15*) had notable effects on plant infection (**Fig. 3**). There are many possible explanations for this. One explanation is that these deleted genes seem not involved in the infection process, as what

seems to be the case for MoMyb8 (Lee et al., 2021). Nevertheless, since all genes are expressed reasonably well in planta at different stages of plant infection (**Table S2**), a more likely explanation is redundancy in function or genetic compensation for most of these gene deletions (El-Brolosy and Stainier, 2017). Similarly regulated genes likely create this redundancy or genetic compensation (**Fig. 8, Fig. S4 and Table S2**). These genes are likely collaborating with the deleted genes at different time points or by upregulation of genes with similarity in amino acid sequence since we found the MoMyb-genes (**Fig. 1A**) sorts into 4 clusters. Of course, the 5 genes we could not delete and that have not been deleted before (*momyb11, 12, 14, 17, and 19*) could also have a role in pathogenicity. If these are truly essential, they naturally have a profound effect on pathogenicity since they might be essential for survival also during infection. Interestingly these potentially essential genes are members of different co-regulated clusters identified (**Fig. 8 and Fig. S4**), making it plausible that they could encode for proteins that act together with the other Myb proteins and take over their functions. That would be a type of genetic compensation often found with knockouts (El-Brolosy and Stainier, 2017).

The gene encoding a Myb protein that affected both growth and infection phenotypes was *MoMyb13*. This protein is large (**Fig. 1A**) and has no orthologues outside Ascomycota. We investigated it further and found similar large proteins predicted in 19 other published genomes (**Fig. 9**). Three of these hits were other strains of *Pyricularia oryzae* (*M. oryzae* teleomorph) which is not strange. Maybe more interesting, common to all hits, including *M.oryzae*, they are all fungi known to produce melanized hydrophobic structures (Collado et al., 2002; Liu et al., 2009; Kokaew et al., 2011; Al-Khawaldeh et al., 2020; Geisen et al., 2021; Sarsaiya et al., 2020; Li et al., 2016; Gao et al., 2021; Chen et al., 2021) indicating that our results showing a possible involvement of MoMyb13 in hydrophobin production could be relevant also for these similar proteins in diverse fungi all belonging to the class Sordariomycetes. Interestingly, all these melanized fungi are also known to grow endophytically, as *M. oryzae* do in the first biotrophic stages of infection (Kankanala et al., 2007) when *MoMyb13* is upregulated (**Fig. 8 and Fig. S4).** Whether these genes and gene products have similar functions as in *M. oryzae* is unknown. Future research should investigate whether these genes could complement *MoMyb13* or each other since *MoMyb13* seems very important in the early stages of *M. oryzae* infection of rice.

The other gene that gave apparent phenotypes when deleted was *MoMyb15*, which encodes for an ISW2 like protein potentially involved in gene regulation by regulating the access of transcription factors by binding to DNA and controlling nucleosome positioning. Thus it regulates the access of DNA to other transcription factors and repressors instead of being a transcription factor itself (Fazzio et al., 2005; Hada et al., 2019; Kagalwala et al., 2004). It would be interesting to study this further and focus on which DNA sequences it binds to (CHP-seq) and the regulatory effect of the deletion on physically adjacent genes in the genome. According to our results (**Fig. 8 and S4 and Table S2**). the *MoMyb15* gene is upregulated at HPIs indicative of the transition from biotrophy to necrotrophy (Kankanala et al., 2007), indicating it could be essential for regulating the fungus defenses against plant defenses that are strongly upregulated during the necrotrophic stage (Kou et al., 2019).

Conclusion

The identified 19 Myb-protein encoding genes are differentially expressed during rice infection. However, we replaced Myb-domain encoding genes with Myb-GFP encoding genes and got a

strong enough GFP signal from all encoded proteins localized to the nucleus predicted for Myb-domain-containing proteins. Thus the 19 *Myb* genes have likely many different and overlapping functions and are, in addition, not all encoding classical DNA binding transcription factors (Prouse and Campbell, 2012) as sometimes implicated (Cao et al., 2020; Dong et al., 2015; Du et al., 2009; Dubos et al., 2010; Li et al., 2019; Liu et al., 2015; Roy, 2016; Verma et al., 2017). Deleting the two genes encoding MoMyb13 and MoMyb15 resulted in phenotypes affecting the pathogenicity of the fungus, and the two genes appeared to be most active at different stages of the plant infection. These two genes should be studied in detail in future experiments for different reasons.

MoMyb13 is active during the biotrophic establishment phase. The orthologues of its gene's products are only present in relatively closely related ascomycetes having biotrophic/endophytic relationships with plants, possibly indicating that they are not this gene and its product has some essential function for establishing biotrophic interactions. This gene product could also potentially be targeted by control measures since it does not seem to be widely spread among fungi outside the class Sordariomycetes.

MoMyb15 is an ISW2 type Myb-containing protein conserved in eukaryotes; it affects local heterochromatin formation and gene expression (Fazzio et al., 2005). Thus, we have initiated detailed research on MoMyb15 to investigate if it has a similar function in *M. oryzae*. The other genes encoding proteins with Myb-domains gave no phenotypes or appeared to be essential. However, these genes should be studied using knockdown systems mutation-induced genetic compensation (El-Brolosy and Stainier, 2017) or conditional knockdown systems for their possibly essential genes.

Acknowledgments

The strain Ku80 used in this study was obtained initially from Nicholas J. Talbot, University of Exeter, UK. This research was financially supported by the National Science Foundation of China (NSFC31871914)

Figure Legends

Figure 1. Domain structure of the identified genes encoding for Myb domain-containing proteins and their phylogenetic relationships. (**A**) Identified conserved domain in the found Myb domain containing proteins. (**B**) Phylogenetic relationship based on similarity of predicted amino acid sequences showed that the 19 proteins could be sorted into 4 groups marked by the color code.

Figure 2. The radial growth rates of *Δmomyb2, Δmomyb13*, and *Δmomyb15* are slower than in the background strain Ku80. (**A**) Images of the morphology of the different strains on the three different media, complete medium (CM), minimal medium (MM), and rice bran medium (RBM). (**B**) Measured colony diameter after 10-day incubation in alternating dark/light (12h/12h) at 25 ^{O}C. (**C**) Growth inhibition in comparison with the background strain Ku80. Bars indicate SEM and bars with the same letters are not significantly different (P>0.05; t-test).

Figure 3. Only MoMyb13 and MoMyb15 appear to be involved in *M. oryzae* pathogenicity on rice as tested by the agar block technique on excised barley and rice leaves since the mutants formed no conidia. (**A**) Test of mutants and background strain on barley leaves. (**B**) Test of mutants and background strain on rice leaves. (**C**) Mycelia appressorium formation from mycelial fragments on a hydrophobic surface.

Figure 4. *Δmomyb13* and *Δmomyb15* form no conidia. (**A**) Conidiophore morphology and conidiation. (**B**) Conidia production on CM and RBM.

Figure 5. Hydrophobin production is affected by the *Δmomyb13* mutation. (A) colonies of *Δmomyb13* are easily wettable, while the surface of the background strain (Ku80), the complementation strain, or the *Δmomyb13* strain containing the overexpressed hydrophobin *MPG1* (*Δmomyb13/TrpC-MPG1* is not easily wettable. (**B**) Expression of 4 hydrophobin genes in *Δmomyb13* showing that *MPG1* is severely downregulated. (**C**) *MPG1* expression in strain Ku80, *Δmomyb13, and Δmomyb13/TrpC-MPG1* strains. (**D**) Upregulation of *MPG1* does not restore the pathogenicity of *Δmomyb13*.

Figure 6. The three mutants, *Δmomyb2, Δmomyb13*, and *Δmomyb15,* showed reduced stress tolerance compared to the background strain Ku80. (**A**) Colony size and morphology Ku80, the mutants, and the complements growing on CM or CM with additions of SDS, CR, NaCl SOR, or H_2O_2 (see methods) after growth for 10 days in alternating dark/light (12h/12h) at 25°C. (**B**) Same as in (**A**) but showing the average of the replicates. Bars indicate the standard error of the respective means.

Figure 7. All three MoMyb proteins that showed apparent phenotypes when deleted (*Δmomyb13*, *Δmomyb2,* and *Δmomyb15*) localize to conidial, appressorial, and mycelial nuclei as indicated by co-localization with the mCherry labeled nuclear marker MoHis1-mCherry. (**A**) MoMyb13-GFP localizes to nuclei. (**B**) MoMyb2-GFP localizes to nuclei and mainly to what is most probably the nucleoli. (**C**) MoMyb15-GFP localizes to the nuclei.

Figure 8. The different *MoMyb* genes show different expression profiles. The MoMyb gene expression profiles cluster into 5 clusters mainly dependent on hours post-infection (HPI) values. This clustering is, in principle, similar to what can be seen in the PCA plot (**Fig. S4**). Transcripts from growth on agar medium (MY), conidia (late in the formation of these), 8 HPI (8h), 24 HPI (24h), 48 HPI (48h), 72 HPI (72h), and 96 HPI (96h). The color code used is the same as in **Fig. 1A** for the phylogeny clusters showing that the regulatory clusters contain sets of genes with little similarity in homology. Ellipses mark the 3 genes with phenotypes different from Ku80 for their respective deletion mutants.

Figure 9. Alignments of highly similar orthologues to the MoMyb13 protein (E-values less or equal 3E-135 and with more than 70% query cover) (**Table S3**). Data from an NCBI produced alignment.

Figure S1. Southern blot confirmation for all the 12 mutants obtained in this study.

Figure S2. Localization of the MoMyb-GFP complements from which we could find strong enough GFP signals.

Figure S3. No change in pathogenicity due to the mutations can be seen for 9 of the 12 mutants tested (**A**) Test of mutants and background strain (Ku80) on barley leaves using the agar block technique (**B**) Test of mutants and background strain (Ku80) conidia sprayed on rice leaves.

Figure S4. The different *MoMyb* genes show different expression profiles visualized by Principal Component Analysis (PCA). Variables were transcription with different treatments and HPIs from infected rice leaves, growth on agar medium (MY), conidia (Conidia late), 8 HPI (8h), 24 HPI (24h), 48 HPI (48h), 72 HPI (72h) and 96 HPI (96h). The expression values of the 19 identified genes encoding Myb domain-containing proteins were the objects. The first and second PCA are presented after a PCA based on the correlation of the expression profiles (as shown in **Fig. S5**). The plot is a biplot also showing the loading of the variables in the two PCs. A minimum spanning tree nearly identical to the tree in Fig. 8 joins the most similar genes in all PCs calculated. The color code used for the markers beside the gene names is the same as in **Fig. 1A** for the phylogeny clusters, showing that the regulatory clusters contain sets of genes with little similarity in sequence homology. An X as a marker indicates a gene we could not delete. Boxes mark the 3 genes with noted phenotypes for their deletion mutants.

Table S1. Primers used in this study

Table S2. List of MoMyb proteins organized after their expression profile similarities.

Table S3. Similarity of NCBI hit data of highly similar orthologues to MoMyb13 (E value less or equal 3E-135) With more than 70% query cover.

References

Al-Khawaldeh, M.M., Araj, S.-E., Alananbeh, K.M., Antary, T.M.A., 2020. WHEAT CULTIVABLE FUNGAL ENDOPHYTES IN JORDAN. Fresenius Environmental Bulletin 29, 13.

Bayry, J., Aimanianda, V., Guijarro, J.I., Sunde, M., Latgé, J.-P., 2012. Hydrophobins—Unique Fungal Proteins. PLoS Pathog 8, e1002700. https://doi.org/10.1371/journal.ppat.1002700

Berger, B.W., Sallada, N.D., 2019. Hydrophobins: multifunctional biosurfactants for interface engineering. J Biol Eng 13, 10. https://doi.org/10.1186/s13036-018-0136-1

Cao, Y., Li, K., Li, Y., Zhao, X., Wang, L., 2020. MYB Transcription Factors as Regulators of Secondary Metabolism in Plants. Biology 9, 61. https://doi.org/10.3390/biology9030061

Chen, H., Mao, L., Zhao, N., Xia, C., Liu, J., Kubicek, C.P., Wu, W., Xu, S., Zhang, C., 2021. Verification of TRI3 Acetylation of Trichodermol to Trichodermin in the Plant Endophyte Trichoderma taxi. Front. Microbiol. 12, 731425. https://doi.org/10.3389/fmicb.2021.731425

Collado, J., Gonzalez, A., Platas, G., Stchigel, A.M., Guarro, J., Pelaez, F., 2002. Monosporascus ibericus sp. nov., an endophytic ascomycete from plants on saline soils, with observations on the position of the genus based on sequence analysis of the 18S rDNA. Mycological Research 106, 118–127. https://doi.org/10.1017/S0953756201005172

Dean, R.A., Talbot, N.J., Ebbole, D.J., Farman, M.L., Mitchell, T.K., Orbach, M.J., Thon, M., Kulkarni, R., Xu, J.-R., Pan, H., Read, N.D., Lee, Y.-H., Carbone, I., Brown, D., Oh, Y.Y., Donofrio, N., Jeong, J.S., Soanes, D.M., Djonovic, S., Kolomiets, E., Rehmeyer, C., Li, W., Harding, M., Kim, S., Lebrun, M.-H., Bohnert, H., Coughlan, S., Butler, J., Calvo, S., Ma, L.-J., Nicol, R., Purcell, S., Nusbaum, C., Galagan, J.E., Birren, B.W., 2005. The genome sequence of the rice blast fungus Magnaporthe grisea. Nature 434, 980–986. https://doi.org/10.1038/nature03449

Dong, Y., Zhao, Q., Liu, X., Zhang, X., Qi, Z., Zhang, H., Zheng, X., Zhang, Z., 2015. MoMyb1 is required for asexual development and tissue-specific infection in the rice blast fungus Magnaporthe oryzae. BMC Microbiol 15, 37. https://doi.org/10.1186/s12866-015-0375-y

Du, H., Zhang, L., Liu, L., Tang, X.-F., Yang, W.-J., Wu, Y.-M., Huang, Y.-B., Tang, Y.-X., 2009. Biochemical and molecular characterization of plant MYB transcription factor family. Biochemistry Moscow 74, 1–11. https://doi.org/10.1134/S0006297909010015

Dubos, C., Stracke, R., Grotewold, E., Weisshaar, B., Martin, C., Lepiniec, L., 2010. MYB transcription factors in Arabidopsis. Trends in Plant Science 15, 573–581. https://doi.org/10.1016/j.tplants.2010.06.005

Ebbole, D.J., 2007. Magnaporthe as a Model for Understanding Host-Pathogen Interactions. Annu. Rev. Phytopathol. 45, 437–456. https://doi.org/10.1146/annurev.phyto.45.062806.094346

El-Brolosy, M.A., Stainier, D.Y.R., 2017. Genetic compensation: A phenomenon in search of mechanisms. PLoS Genet 13, e1006780. https://doi.org/10.1371/journal.pgen.1006780

Eme, L., Spang, A., Lombard, J., Stairs, C.W., Ettema, T.J.G., 2017. Archaea and the origin of eukaryotes. Nat Rev Microbiol 15, 711–723. https://doi.org/10.1038/nrmicro.2017.133

Fazzio, T.G., Gelbart, M.E., Tsukiyama, T., 2005. Two Distinct Mechanisms of Chromatin Interaction by the Isw2 Chromatin Remodeling Complex In Vivo. Mol Cell Biol 25, 9165–9174. https://doi.org/10.1128/MCB.25.21.9165-9174.2005

Gao, H., Pan, M., Tian, C., Fan, X., 2021. Cytospora and Diaporthe Species Associated With Hazelnut Canker and Dieback in Beijing, China. Front. Cell. Infect. Microbiol. 11, 664366. https://doi.org/10.3389/fcimb.2021.664366

Geisen, S., Hooven, F.C., Kostenko, O., Snoek, L.B., Putten, W.H., 2021. Fungal root endophytes influence plants in a species-specific manner that depends on plant's growth stage. J Ecol 109, 1618–1632. https://doi.org/10.1111/1365-2745.13584

Gladieux, P., Condon, B., Ravel, S., Soanes, D., Maciel, J.L.N., Nhani, A., Chen, L., Terauchi, R., Lebrun, M.-H., Tharreau, D., Mitchell, T., Pedley, K.F., Valent, B., Talbot, N.J., Farman, M., Fournier, E., 2018. Gene Flow between Divergent Cereal- and Grass-Specific Lineages of the Rice Blast Fungus *Magnaporthe oryzae*. mBio 9. https://doi.org/10.1128/mBio.01219-17

Hada, A., Hota, S.K., Luo, J., Lin, Y., Kale, S., Shaytan, A.K., Bhardwaj, S.K., Persinger, J., Ranish, J., Panchenko, A.R., Bartholomew, B., 2019. Histone Octamer Structure Is Altered Early in ISW2 ATP-Dependent Nucleosome Remodeling. Cell Reports 28, 282-294.e6. https://doi.org/10.1016/j.celrep.2019.05.106

Hammer, O., Harper, D.A.T., Ryan, P.D., 2001. PAST: Paleontological Statistics Software Package for Education and Data Analysis 4, 9.

Howard, R.J., Ferrari, M.A., Roach, D.H., Money, N.P., 1991. Penetration of hard substrates by a fungus employing enormous turgor pressures. Proceedings of the National Academy of Sciences 88, 11281–11284. https://doi.org/10.1073/pnas.88.24.11281

Islam, M.T., Croll, D., Gladieux, P., Soanes, D.M., Persoons, A., Bhattacharjee, P., Hossain, Md.S., Gupta, D.R., Rahman, Md.M., Mahboob, M.G., Cook, N., Salam, M.U., Surovy, M.Z., Sancho, V.B., Maciel, J.L.N., NhaniJúnior, A., Castroagudín, V.L., Reges, J.T. de A., Ceresini, P.C., Ravel, S., Kellner, R., Fournier, E., Tharreau, D., Lebrun, M.-H., McDonald, B.A., Stitt, T., Swan, D., Talbot, N.J., Saunders, D.G.O., Win, J., Kamoun, S., 2016. Emergence of wheat blast in Bangladesh was caused by a South American lineage of Magnaporthe oryzae. BMC Biol 14, 84. https://doi.org/10.1186/s12915-016-0309-7

Kagalwala, M.N., Glaus, B.J., Dang, W., Zofall, M., Bartholomew, B., 2004. Topography of the ISW2–nucleosome complex: insights into nucleosome spacing and chromatin remodeling. EMBO J 23, 2092–2104. https://doi.org/10.1038/sj.emboj.7600220

Kankanala, P., Czymmek, K., Valent, B., 2007. Roles for Rice Membrane Dynamics and Plasmodesmata during Biotrophic Invasion by the Blast Fungus. The Plant Cell 19, 706–724. https://doi.org/10.1105/tpc.106.046300

Kokaew, J., Manoch, L., Worapong, J., Chamswarng, C., Singburaudom, N., Visarathanonth, N., Piasai, O., Strobel, G., 2011. Coniochaeta ligniaria an Endophytic Fungus from Baeckea frutescens and Its Antagonistic Effects Against Plant Pathogenic Fungi 44, 9.

Kou, Y., Qiu, J., Tao, Z., 2019. Every Coin Has Two Sides: Reactive Oxygen Species during Rice–Magnaporthe oryzae Interaction. IJMS 20, 1191. https://doi.org/10.3390/ijms20051191

Lee, S., Völz, R., Song, H., Harris, W., Lee, Y.-H., 2021. Characterization of the MYB Genes Reveals Insights Into Their Evolutionary Conservation, Structural Diversity, and Functional Roles in Magnaporthe oryzae. Front. Microbiol. 12, 721530. https://doi.org/10.3389/fmicb.2021.721530

Li, H., Lu, J., Liu, X., Xhang, L., Lin, F., 2012. Vector Building and Usage for Gene Knockout, Protein Expression and Fluorescent Fusion Protein in The Rice Blast Fungus. Journal of

Agricultural Biotechnology 20, 94–104. https://doi.org/10.3969/j.issn.1674-7968.2012.01.013

Li, J., Han, G., Sun, C., Sui, N., 2019. Research advances of MYB transcription factors in plant stress resistance and breeding. Plant Signaling & Behavior 14, 1613131. https://doi.org/10.1080/15592324.2019.1613131

Li, T., Wang, X., Luo, J., Yang, M., Kong, L., 2016. Antioxidant sordariol dimers from Sordaria macrospora and the absolute configuration determinations of their two simultaneous linear 1,2-diols. Tetrahedron Letters 57, 2754–2757. https://doi.org/10.1016/j.tetlet.2016.05.014

Li, Y., Liang, S., Yan, X., Wang, H., Li, D., Soanes, D.M., Talbot, N.J., Wang, Zonghua, Wang, Zhengyi, 2010a. Characterization of *MoLDB1* Required for Vegetative Growth, Infection-Related Morphogenesis, and Pathogenicity in the Rice Blast Fungus *Magnaporthe oryzae*. MPMI 23, 1260–1274. https://doi.org/10.1094/MPMI-03-10-0052

Li, Y., Que, Y., Liu, Y., Yue, X., Meng, X., Zhang, Z., Wang, Z., 2015. The putative Gγ subunit gene MGG1 is required for conidiation, appressorium formation, mating and pathogenicity in Magnaporthe oryzae. Curr Genet 61, 641–651. https://doi.org/10.1007/s00294-015-0490-1

Li, Y., Yan, X., Wang, H., Liang, S., Ma, W.-B., Fang, M.-Y., Talbot, N.J., Wang, Z.-Y., 2010b. MoRic8 Is a Novel Component of G-Protein Signaling During Plant Infection by the Rice Blast Fungus *Magnaporthe oryzae*. MPMI 23, 317–331. https://doi.org/10.1094/MPMI-23-3-0317

Li, Y., Yue, X., Que, Y., Yan, X., Ma, Z., Talbot, N.J., Wang, Z., 2014. Characterisation of Four LIM Protein-Encoding Genes Involved in Infection-Related Development and Pathogenicity by the Rice Blast Fungus Magnaporthe oryzae. PLoS ONE 9, e88246. https://doi.org/10.1371/journal.pone.0088246

Liu, J., Osbourn, A., Ma, P., 2015. MYB Transcription Factors as Regulators of Phenylpropanoid Metabolism in Plants. Molecular Plant 8, 689–708. https://doi.org/10.1016/j.molp.2015.03.012

Liu, K., Ding, X., Deng, B., Chen, W., 2009. Isolation and characterization of endophytic taxol-producing fungi from Taxus chinensis. J Ind Microbiol Biotechnol 36, 1171–1177. https://doi.org/10.1007/s10295-009-0598-8

Livak, K.J., Schmittgen, T.D., 2001. Analysis of Relative Gene Expression Data Using Real-Time Quantitative PCR and the 2−ΔΔCT Method. Methods 25, 402–408. https://doi.org/10.1006/meth.2001.1262

Malaker, P.K., Barma, N.C.D., Tiwari, T.P., Collis, W.J., Duveiller, E., Singh, P.K., Joshi, A.K., Singh, R.P., Braun, H.-J., Peterson, G.L., Pedley, K.F., Farman, M.L., Valent, B., 2016. First Report of Wheat Blast Caused by *Magnaporthe oryzae* Pathotype *triticum* in Bangladesh. Plant Disease 100, 2330–2330. https://doi.org/10.1094/PDIS-05-16-0666-PDN

Pennisi, E., 2010. Armed and Dangerous. Science 327, 804–805. https://doi.org/10.1126/science.327.5967.804

Prouse, M.B., Campbell, M.M., 2012. The interaction between MYB proteins and their target DNA binding sites. Biochimica et Biophysica Acta (BBA) - Gene Regulatory Mechanisms 1819, 67–77. https://doi.org/10.1016/j.bbagrm.2011.10.010

Roy, S., 2016. Function of MYB domain transcription factors in abiotic stress and epigenetic

control of stress response in plant genome. Plant Signaling & Behavior 11, e1117723. https://doi.org/10.1080/15592324.2015.1117723

Sakulkoo, W., Osés-Ruiz, M., Oliveira Garcia, E., Soanes, D.M., Littlejohn, G.R., Hacker, C., Correia, A., Valent, B., Talbot, N.J., 2018. A single fungal MAP kinase controls plant cell-to-cell invasion by the rice blast fungus. Science 359, 1399–1403. https://doi.org/10.1126/science.aaq0892

Sarsaiya, S., Jain, A., Fan, X., Jia, Q., Xu, Q., Shu, F., Zhou, Q., Shi, J., Chen, J., 2020. New Insights into Detection of a Dendrobine Compound From a Novel Endophytic Trichoderma longibrachiatum Strain and Its Toxicity Against Phytopathogenic Bacteria. Front. Microbiol. 11, 337. https://doi.org/10.3389/fmicb.2020.00337

Verma, S., Gazara, R.K., Verma, P.K., 2017. Transcription Factor Repertoire of Necrotrophic Fungal Phytopathogen Ascochyta rabiei: Predominance of MYB Transcription Factors As Potential Regulators of Secretome. Front. Plant Sci. 8, 1037. https://doi.org/10.3389/fpls.2017.01037

Villalba, F., Collemare, J., Landraud, P., Lambou, K., Brozek, V., Cirer, B., Morin, D., Bruel, C., Beffa, R., Lebrun, M.-H., 2008. Improved gene targeting in Magnaporthe grisea by inactivation of MgKU80 required for non-homologous end joining. Fungal Genetics and Biology 45, 68–75. https://doi.org/10.1016/j.fgb.2007.06.006

Wang, L., Gao, W., Wu, X., Zhao, M., Qu, J., Huang, C., Zhang, J., 2018. Genome-Wide Characterization and Expression Analyses of Pleurotus ostreatus MYB Transcription Factors during Developmental Stages and under Heat Stress Based on de novo Sequenced Genome. IJMS 19, 2052. https://doi.org/10.3390/ijms19072052

Zhang, L., Zhang, D., Chen, Y., Ye, W., Lin, Q., Lu, G., Ebbole, D.J., Olsson, S., Wang, Z., 2019. Magnaporthe oryzae CK2 Accumulates in Nuclei, Nucleoli, at Septal Pores and Forms a Large Ring Structure in Appressoria, and Is Involved in Rice Blast Pathogenesis. Frontiers in Cellular and Infection Microbiology 9, 113. https://doi.org/10.3389/fcimb.2019.00113

Figures

Figure 1.

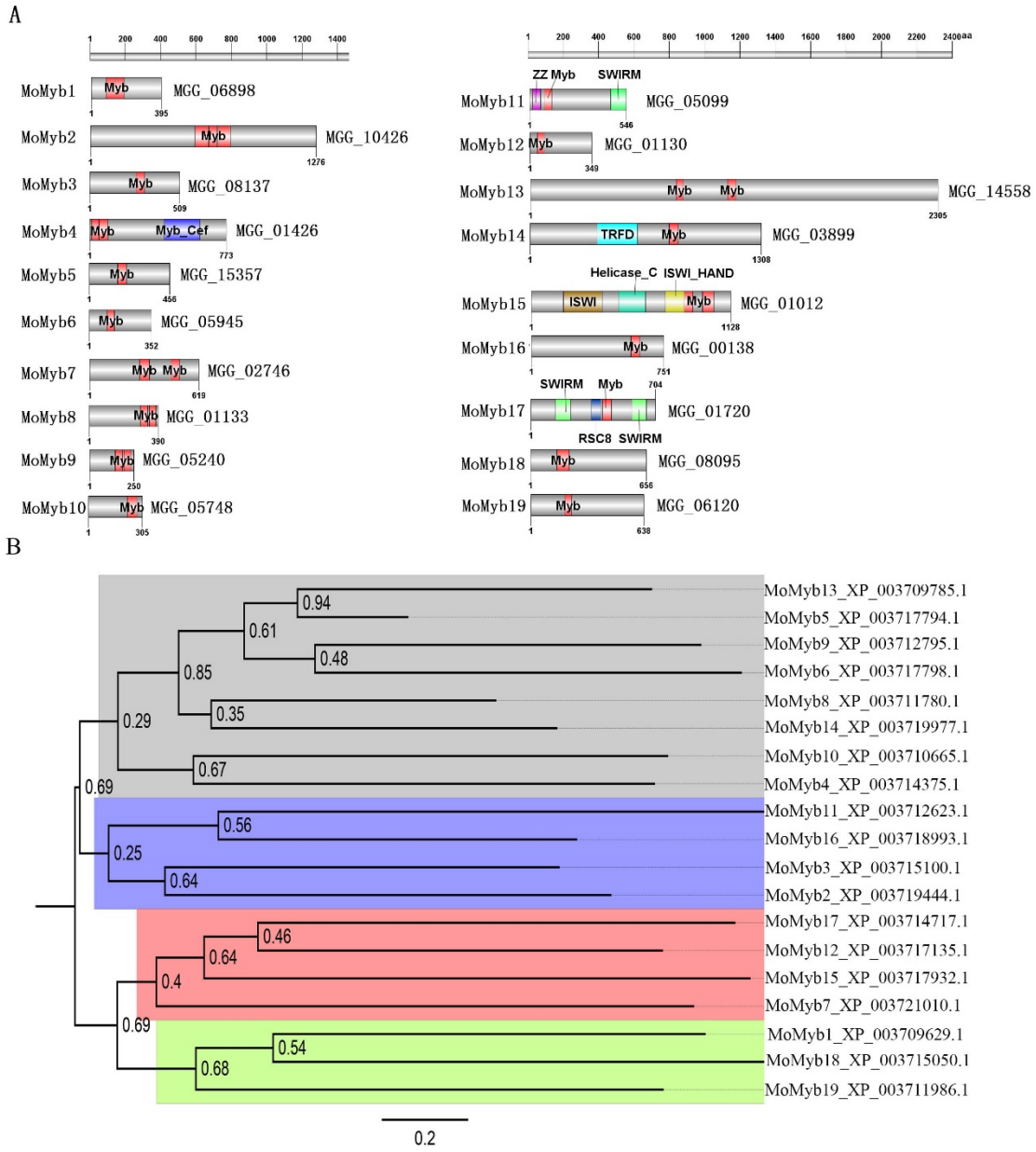

Figure 2

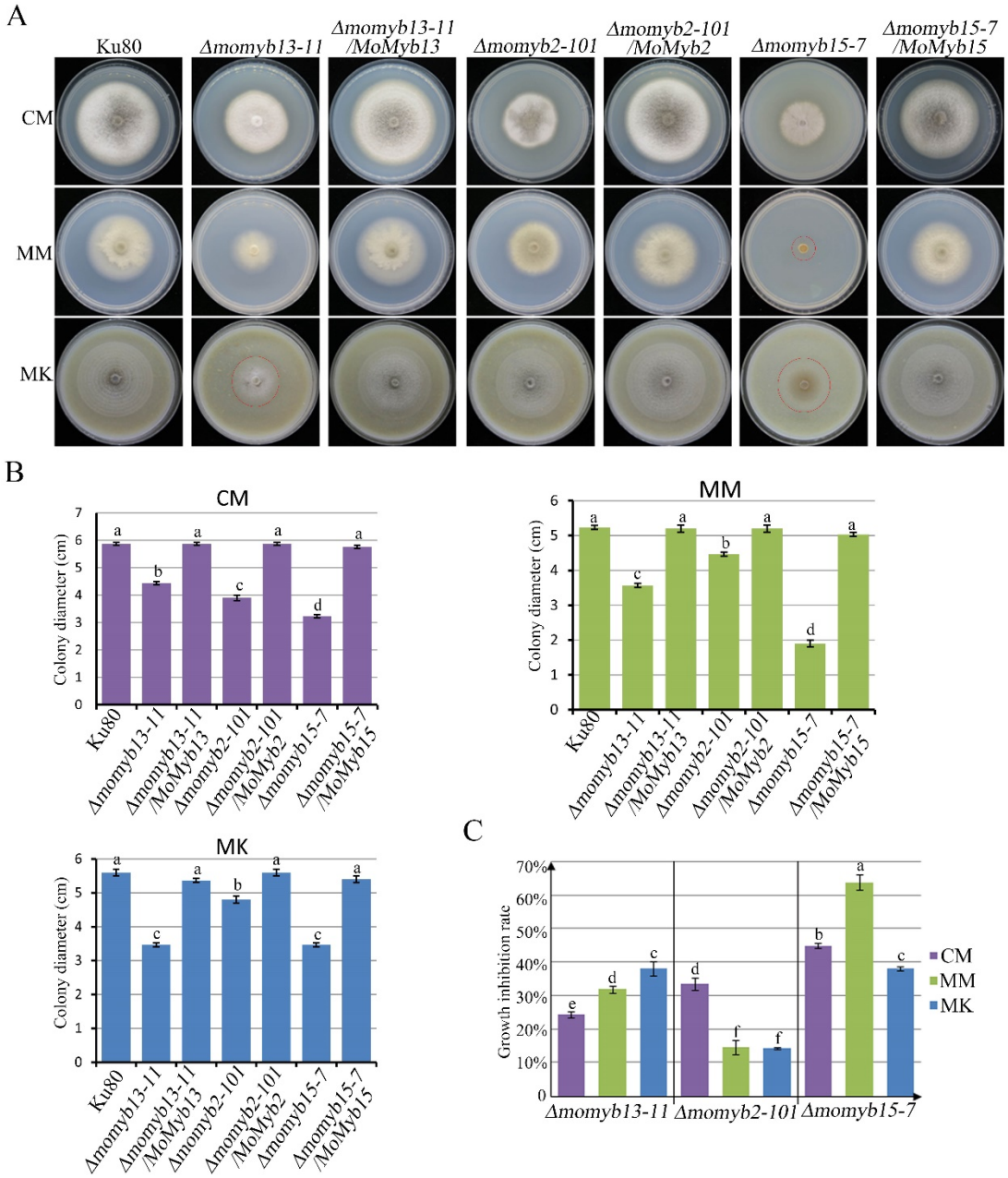
A
Ku80
Δmomyb13-11
Δmomyb13-11 /MoMyb13
Δmomyb2-101
Δmomyb2-101 /MoMyb2
Δmomyb15-7
Δmomyb15-7 /MoMyb15
CM
MM
MK
B
CM
MM
MK
Colony diameter (cm)
Ku80
Δmomyb13-11
Δmomyb13-11 /MoMyb13
Δmomyb2-101
Δmomyb2-101 /MoMyb2
Δmomyb15-7
Δmomyb15-7 /MoMyb15
C
Growth inhibition rate
Δmomyb13-11
Δmomyb2-101
Δmomyb15-7
CM
MM
MK

Figure 3

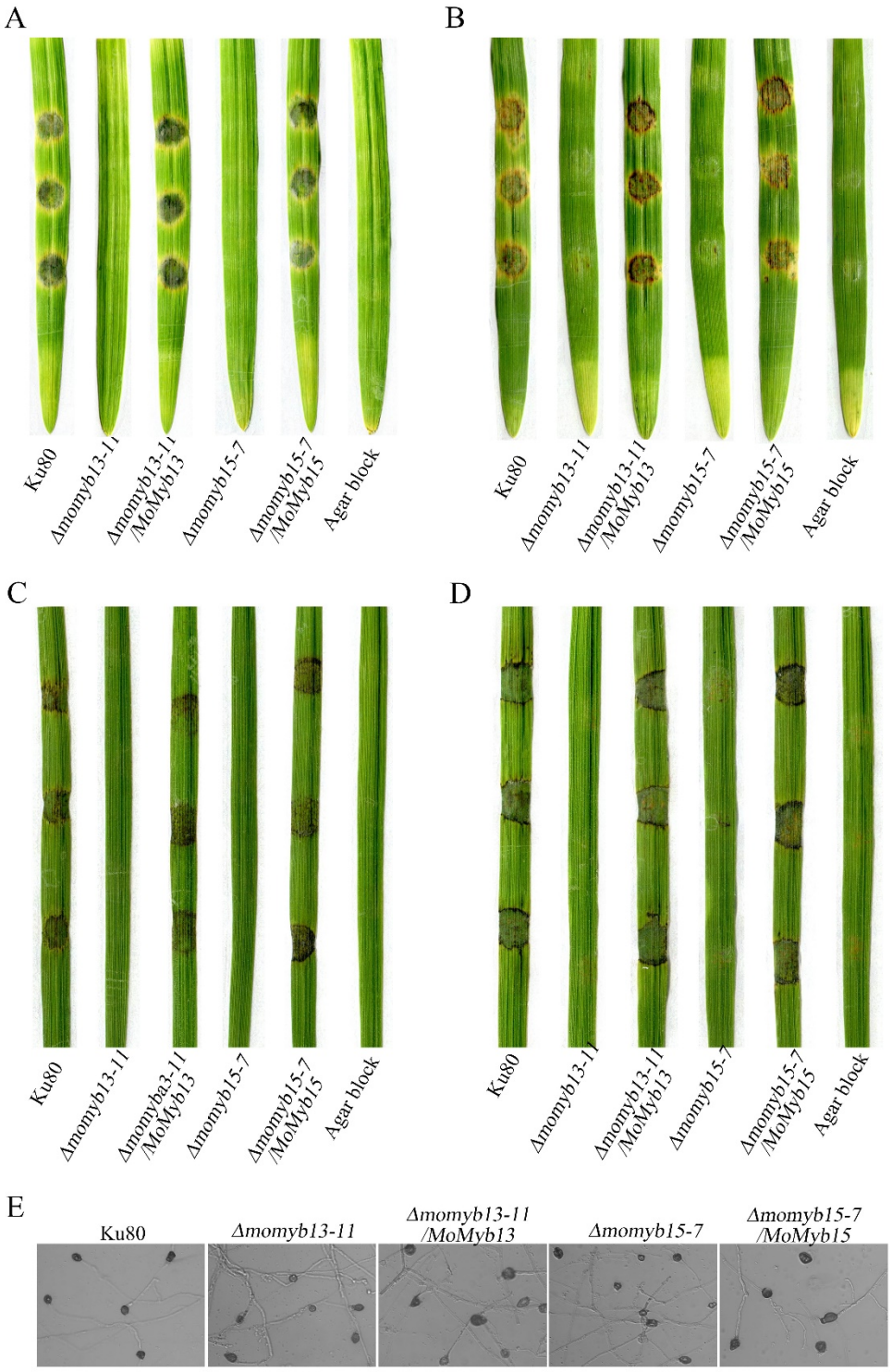
A
Ku80
Δmomyb13-11
Δmomyb13-11 /MoMyb13
Δmomyb15-7
Δmomyb15-7 /MoMyb15
Agar block
B
Ku80
Δmomyb13-11
Δmomyb13-11 /MoMyb13
Δmomyb15-7
Δmomyb15-7 /MoMyb15
Agar block
C
Ku80
Δmomyb13-11
Δmomyba3-11 /MoMyb13
Δmomyb15-7
Δmomyb15-7 /MoMyb15
Agar block
D
Ku80
Δmomyb13-11
Δmomyb13-11 /MoMyb13
Δmomyb15-7
Δmomyb15-7 /MoMyb15
Agar block
E
Ku80
Δmomyb13-11
Δmomyb13-11 /MoMyb13
Δmomyb15-7
Δmomyb15-7 /MoMyb15

Figure 4

A

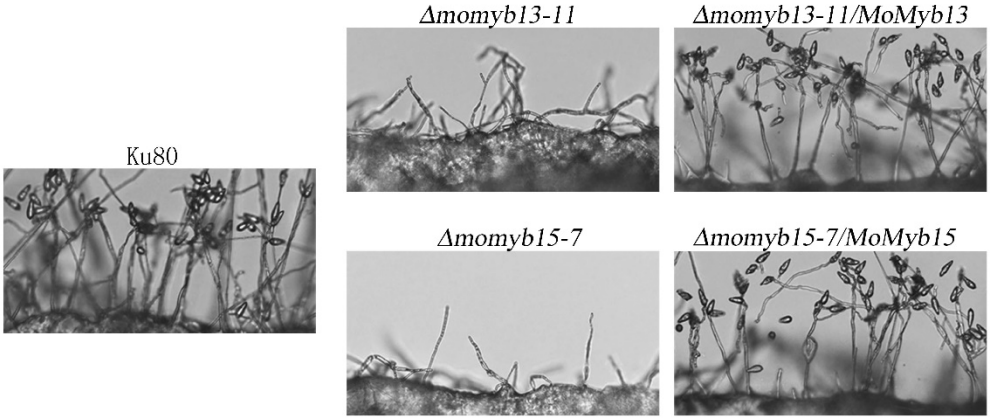
Ku80
Δmomyb13-11
Δmomyb13-11/MoMyb13
Δmomyb15-7
Δmomyb15-7/MoMyb15

B

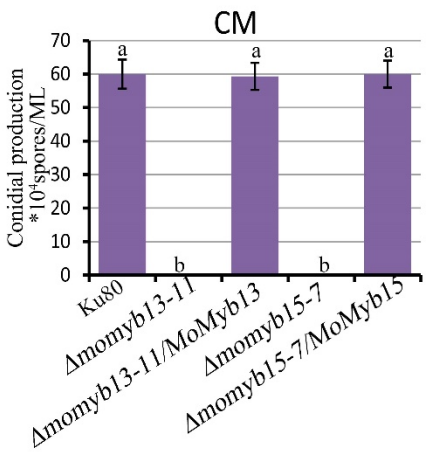
CM
Conidial production
*10⁴spores/ML
70
60
50
40
30
20
10
0
a
b
a
b
a
Ku80
Δmomyb13-11
Δmomyb13-11/MoMyb13
Δmomyb15-7
Δmomyb15-7/MoMyb15

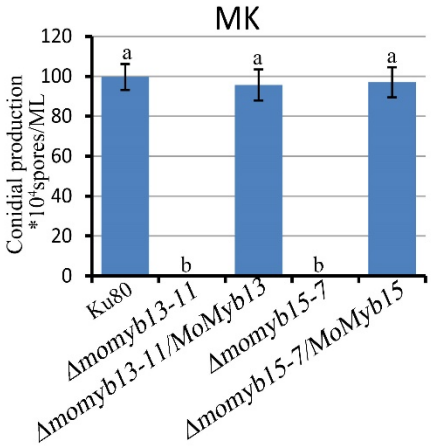
MK
Conidial production
*10⁴spores/ML
120
100
80
60
40
20
0
a
b
a
b
a
Ku80
Δmomyb13-11
Δmomyb13-11/MoMyb13
Δmomyb15-7
Δmomyb15-7/MoMyb15

Figure 5

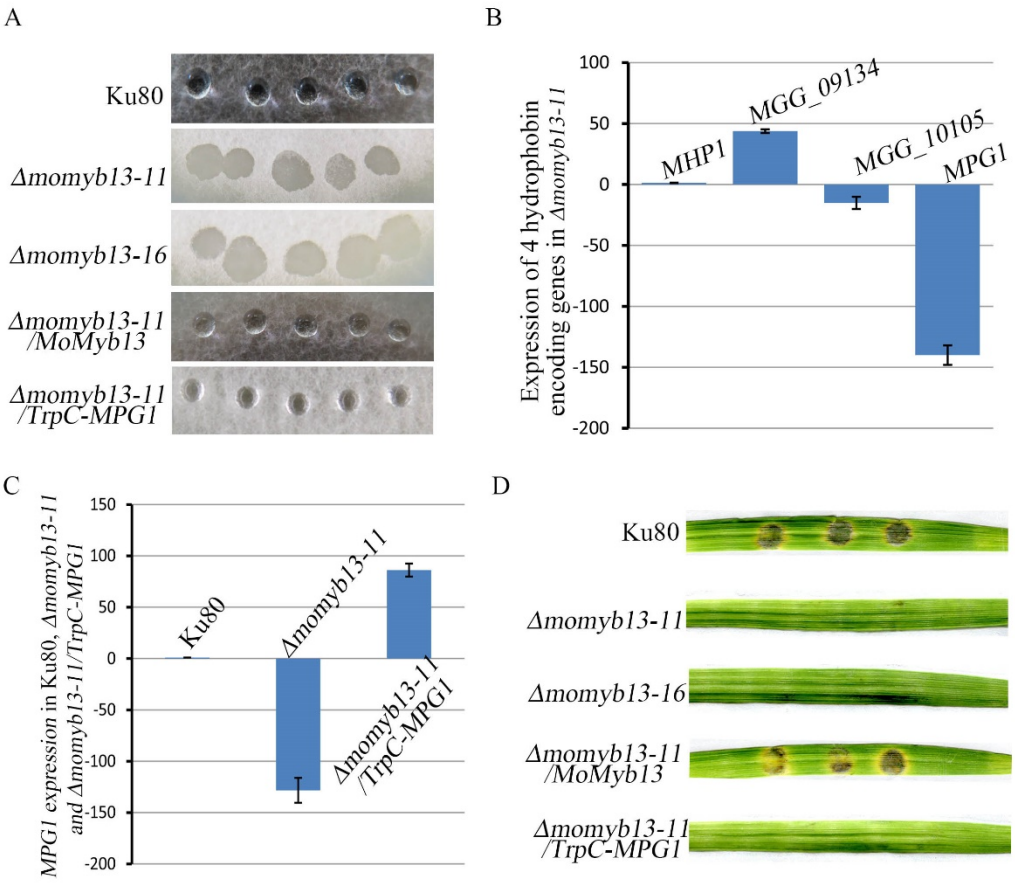
A
Ku80
Δmomyb13-11
Δmomyb13-16
Δmomyb13-11 /MoMyb13
Δmomyb13-11 /TrpC-MPG1
B
Expression of 4 hydrophobin encoding genes in Δmomyb13-11
100
50
0
-50
-100
-150
-200
MHP1
MGG_09134
MGG_10105
MPG1
C
MPG1 expression in Ku80, Δmomyb13-11 and Δmomyb13-11/TrpC-MPG1
150
100
50
0
-50
-100
-150
-200
Ku80
Δmomyb13-11
Δmomyb13-11 /TrpC-MPG1
D
Ku80
Δmomyb13-11
Δmomyb13-16
Δmomyb13-11 /MoMyb13
Δmomyb13-11 /TrpC-MPG1

Figure 6

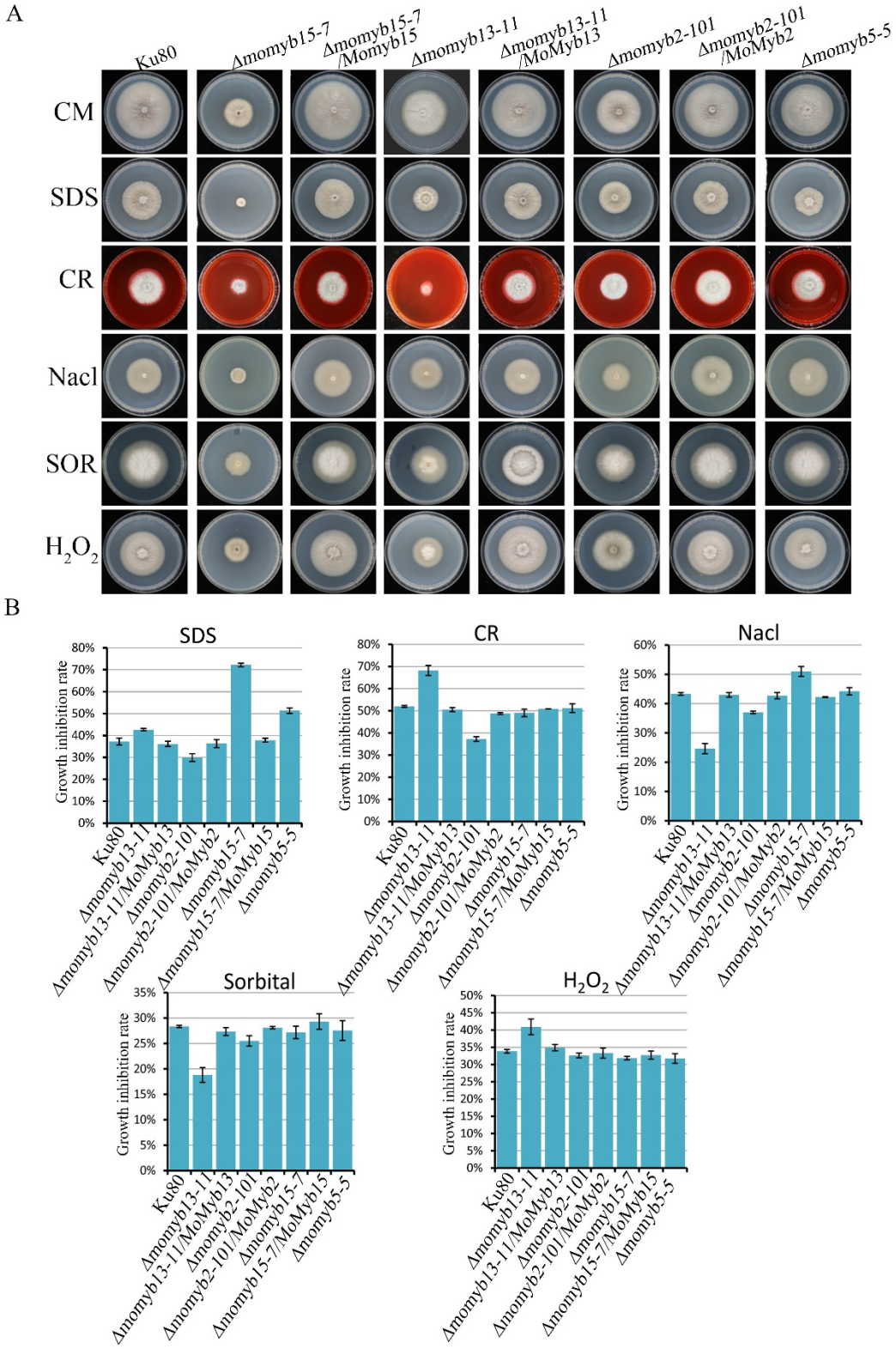
A
Ku80
Δmomyb15-7
Δmomyb15-7 /Momyb15
Δmomyb13-11
Δmomyb13-11 /MoMyb13
Δmomyb2-101
Δmomyb2-101 /MoMyb2
Δmomyb5-5
CM
SDS
CR
Nacl
SOR
H_2O_2
B
SDS
CR
Nacl
Sorbital
H_2O_2
Growth inhibition rate
Ku80
Δmomyb13-11
Δmomyb13-11/MoMyb13
Δmomyb2-101
Δmomyb2-101/MoMyb2
Δmomyb15-7
Δmomyb15-7/MoMyb15
Δmomyb5-5

Figure 7

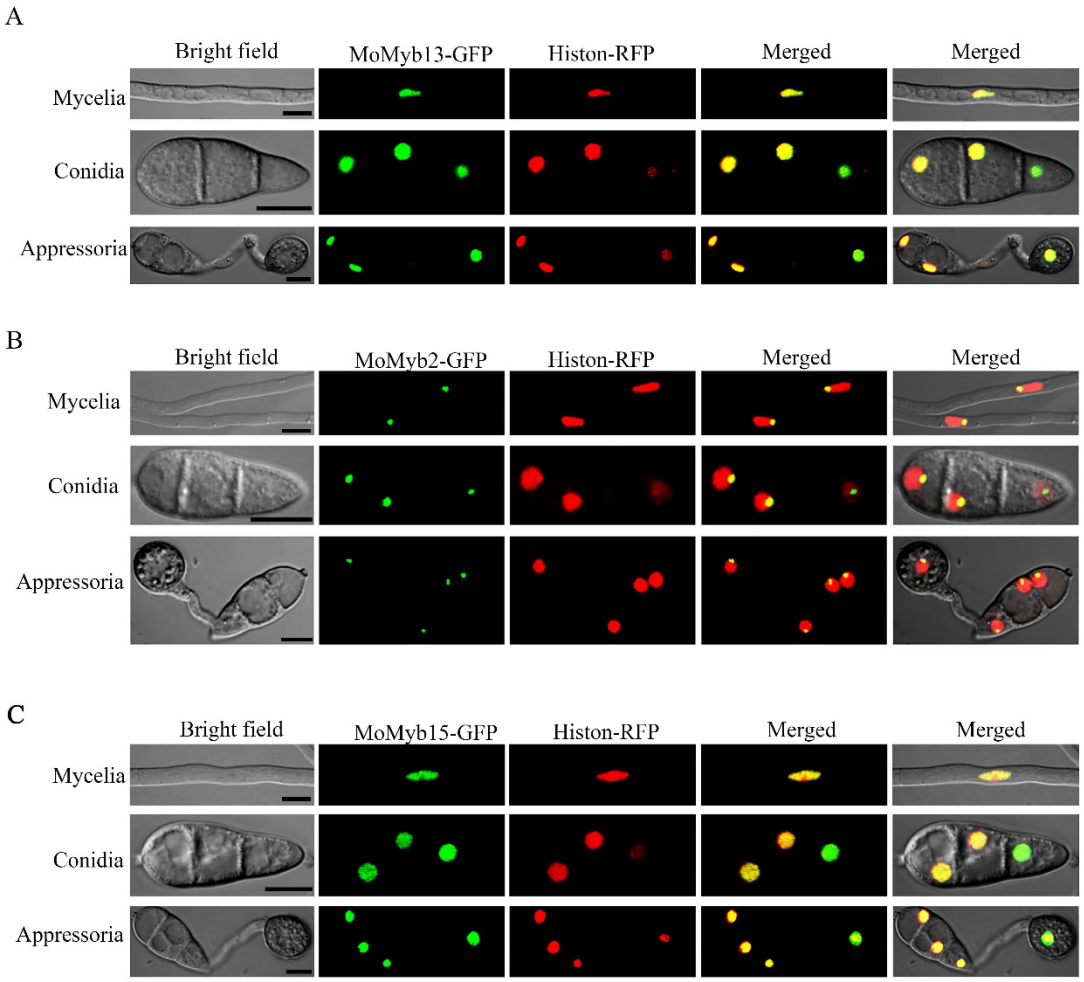
A
Bright field
MoMyb13-GFP
Histon-RFP
Merged
Merged
Mycelia
Conidia
Appressoria
B
Bright field
MoMyb2-GFP
Histon-RFP
Merged
Merged
Mycelia
Conidia
Appressoria
C
Bright field
MoMyb15-GFP
Histon-RFP
Merged
Merged
Mycelia
Conidia
Appressoria

Figure 8

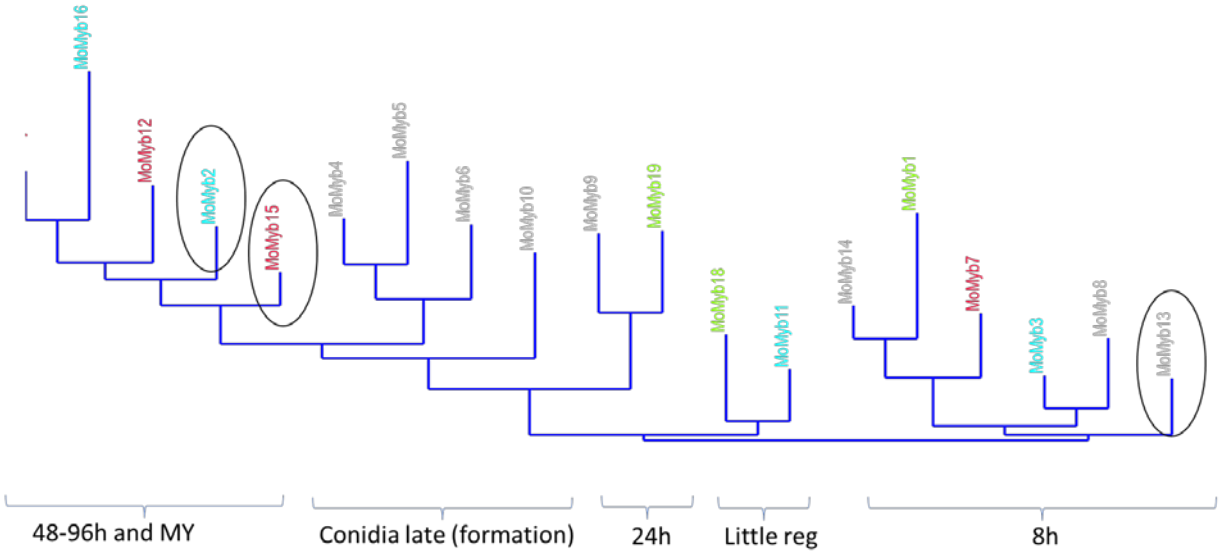
MoMyb16
MoMyb12
MoMyb2
MoMyb15
MoMyb4
MoMyb5
MoMyb6
MoMyb10
MoMyb9
MoMyb19
MoMyb18
MoMyb11
MoMyb14
MoMyb1
MoMyb7
MoMyb3
MoMyb8
MoMyb13
48-96h and MY
Conidia late (formation)
24h
Little reg
8h

Figure 9

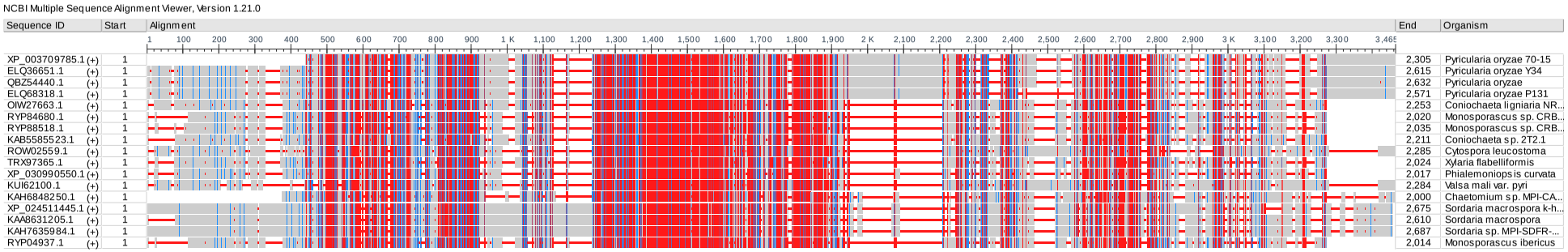
NCBI Multiple Sequence Alignment Viewer, Version 1.21.0
Sequence ID
Start
Alignment
End
Organism
XP_003709785.1 (+) 1 2,305 Pyricularia oryzae 70-15
ELQ36651.1 (+) 1 2,615 Pyricularia oryzae Y34
QBZ54440.1 (+) 1 2,632 Pyricularia oryzae
ELQ68318.1 (+) 1 2,571 Pyricularia oryzae P131
OIW27663.1 (+) 1 2,253 Coniochaeta ligniaria NR...
RYP84680.1 (+) 1 2,020 Monosporascus sp. CRB...
RYP88518.1 (+) 1 2,035 Monosporascus sp. CRB...
KAB5585523.1 (+) 1 2,211 Coniochaeta sp. 2T2.1
ROW02559.1 (+) 1 2,285 Cytospora leucostoma
TRX97365.1 (+) 1 2,024 Xylaria flabelliformis
XP_030990550.1 (+) 1 2,017 Phialemoniopsis curvata
KUI62100.1 (+) 1 2,284 Valsa mali var. pyri
KAH6848250.1 (+) 1 2,000 Chaetomium sp. MPI-CA...
XP_024511445.1 (+) 1 2,675 Sordaria macrospora k-h...
KAA8631205.1 (+) 1 2,610 Sordaria macrospora
KAH7635984.1 (+) 1 2,687 Sordaria sp. MPI-SDFR-...
RYP04937.1 (+) 1 2,014 Monosporascus ibericus

Figure S1

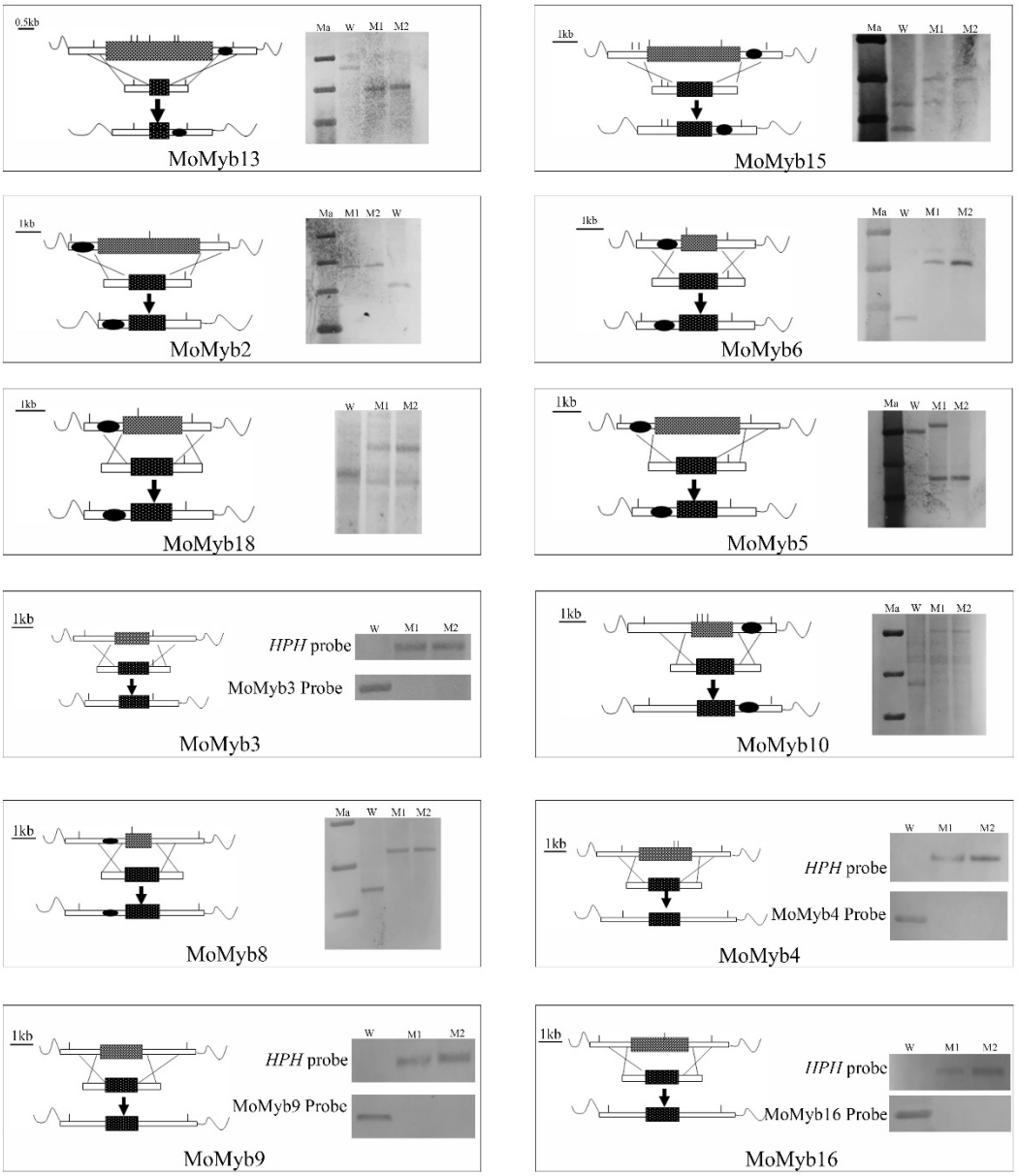

W, Wildtype strain; M1 and M2, 1st and 2rd mutant of the target gene; Ma, Mark.

Figure S2

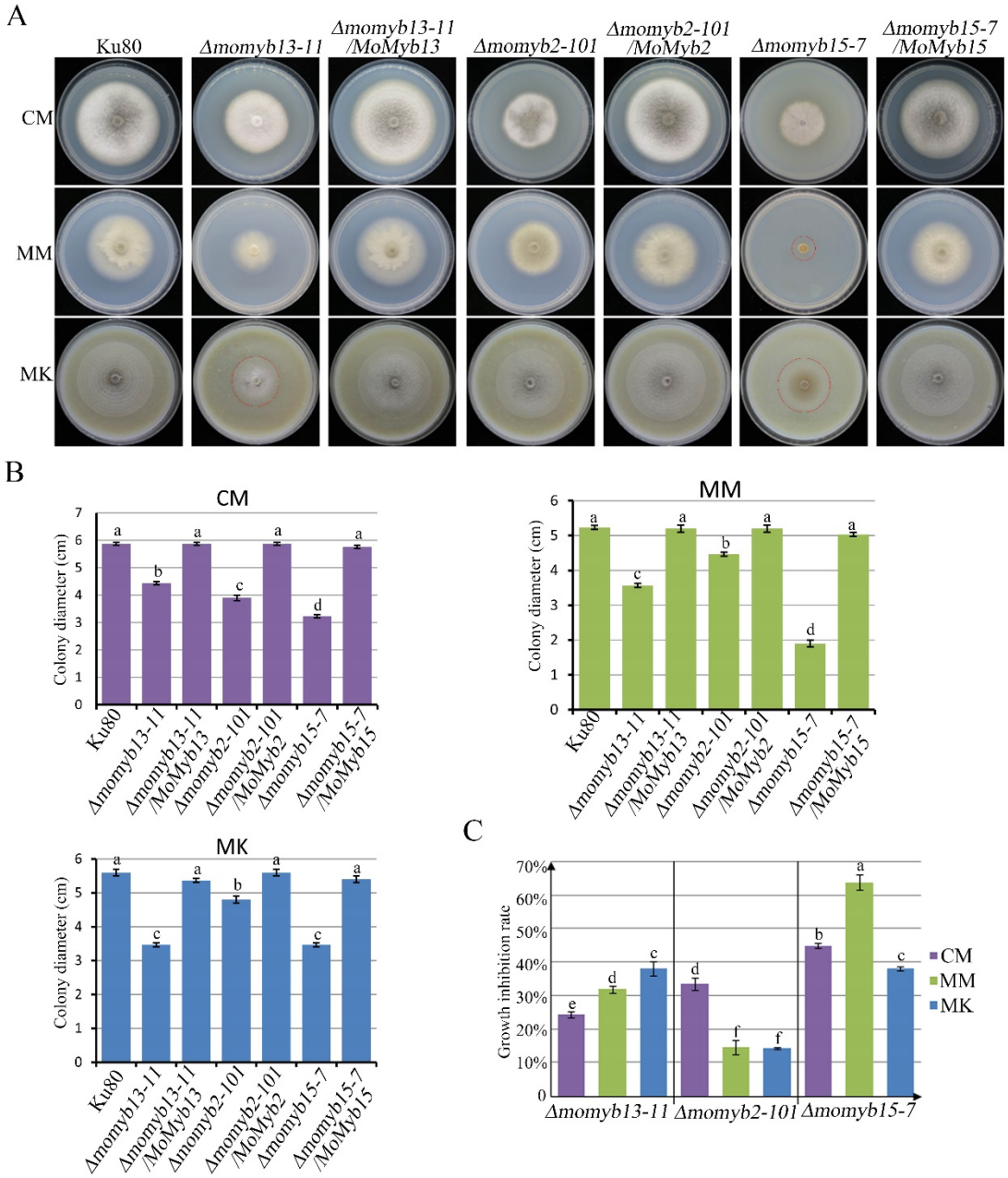
A
Ku80
Δmomyb13-11
Δmomyb13-11 /MoMyb13
Δmomyb2-101
Δmomyb2-101 /MoMyb2
Δmomyb15-7
Δmomyb15-7 /MoMyb15
CM
MM
MK
B
CM
MM
MK
Colony diameter (cm)
Ku80
Δmomyb13-11
Δmomyb13-11 /MoMyb13
Δmomyb2-101
Δmomyb2-101 /MoMyb2
Δmomyb15-7
Δmomyb15-7 /MoMyb15
C
Growth inhibition rate
Δmomyb13-11
Δmomyb2-101
Δmomyb15-7
CM
MM
MK

Figure S3

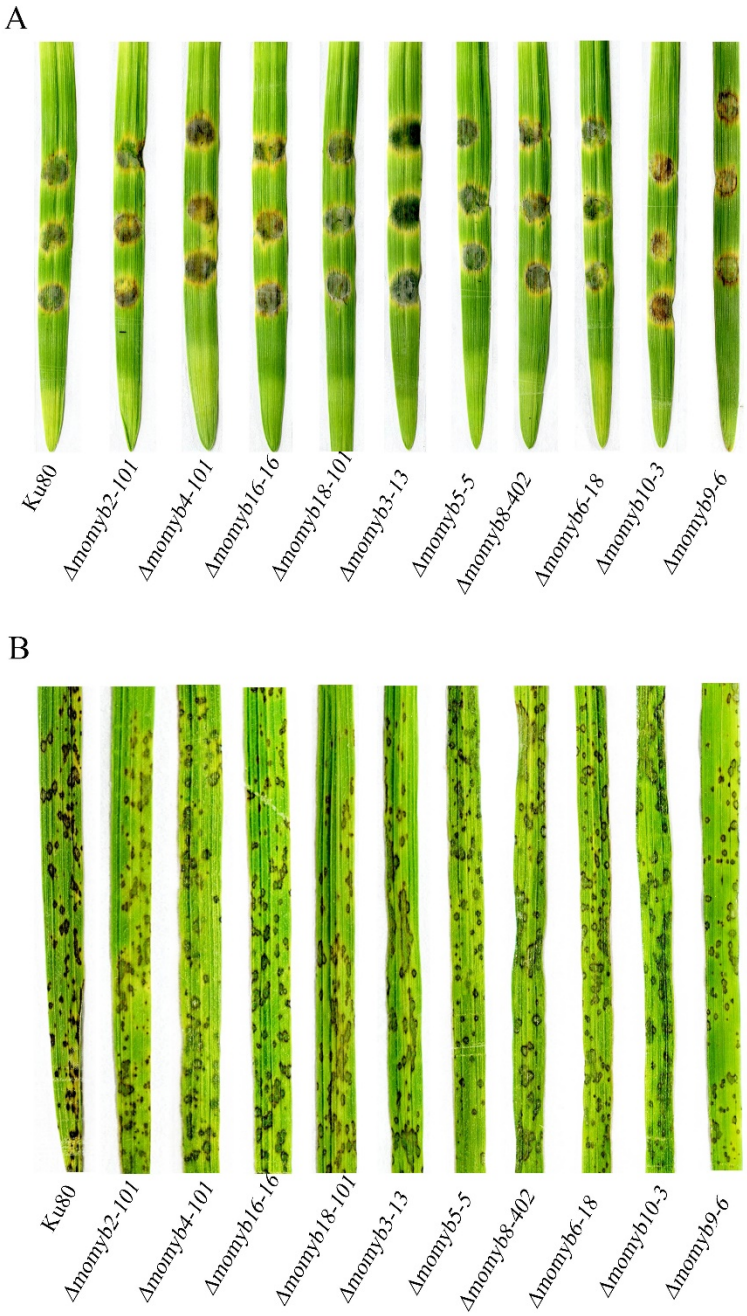
A
Ku80
Δmomyb2-101
Δmomyb4-101
Δmomyb16-16
Δmomyb18-101
Δmomyb3-13
Δmomyb5-5
Δmomyb8-402
Δmomyb6-18
Δmomyb10-3
Δmomyb9-6
B
Ku80
Δmomyb2-101
Δmomyb4-101
Δmomyb16-16
Δmomyb18-101
Δmomyb3-13
Δmomyb5-5
Δmomyb8-402
Δmomyb6-18
Δmomyb10-3
Δmomyb9-6

Figure S4

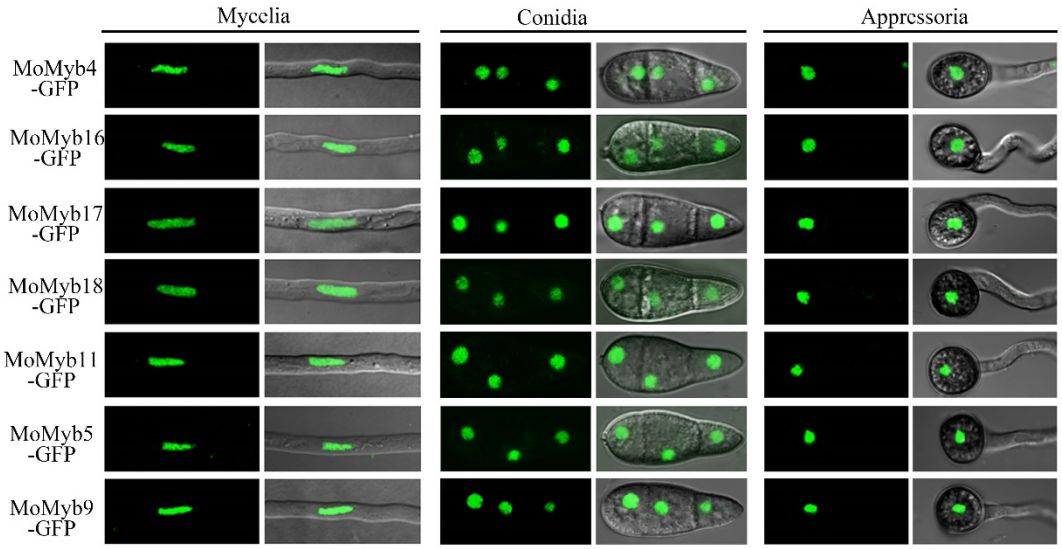
Mycelia
Conidia
Appressoria
MoMyb4
-GFP
MoMyb16
-GFP
MoMyb17
-GFP
MoMyb18
-GFP
MoMyb11
-GFP
MoMyb5
-GFP
MoMyb9
-GFP

Figure S5

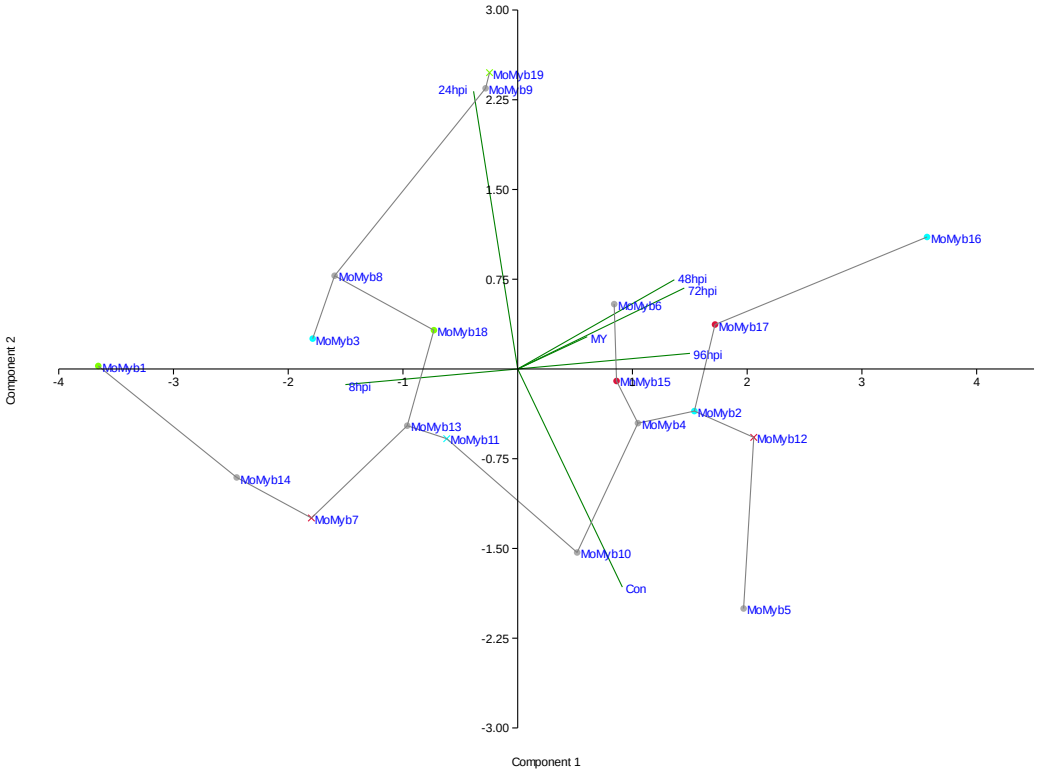
3.00
2.25
1.50
0.75
-0.75
-1.50
-2.25
-3.00
-4
-3
-2
-1
2
3
4
Component 1
Component 2
MoMyb19
MoMyb9
24hpi
MoMyb16
MoMyb8
48hpi
72hpi
MoMyb6
MoMyb17
MoMyb18
MoMyb3
MY
96hpi
MoMyb1
8hpi
MoMyb15
MoMyb2
MoMyb4
MoMyb12
MoMyb13
MoMyb11
MoMyb14
MoMyb7
MoMyb10
Con
MoMyb5

Table S1

Table S1. Primers used in this study

Name	Sequences	Application
MGG_01720-UP-F	aagggaacaaaagctggtaccttctctgggagaccctgttg	Gene deletion
MGG_01720-UP-R	tcagttaacgtcgacaagctttgtggttgtagggtgtcgaa	Gene deletion
MGG_01720-down-F	cgggaaccagttaacctgcagtttgcactacgtcagggaga	Gene deletion
MGG_01720-down-R	cgctctagaactagtggatcccgcttacagtgcttgttgga	Gene deletion
MGG_01012-UP-F	aagggaacaaaagctggtaccACGGCTTGACGGTTACTTGT	Gene deletion
MGG_01012-UP-R	tcagttaacgtcgacaagcttTTGTCGTGAGATTCCCTGGT	Gene deletion
MGG_01012-down-F	cgggaaccagttaacctgcagGTTTGGAACTCTTTGATGGG	Gene deletion
MGG_01012-down-R	cgctctagaactagtggatccGGGCTACTTTGACTTTATGT	Gene deletion
pCB1532-MGG_01012-Pro-F	cgctctagaactagtggatccAGGTGGATGATGTCGATTGCC	Gene complementation
pCB1532-MGG_01012-EcoR1	gcccttgctcaccatgaattcTTTCTTCTTGCCCTTGGCC	Gene complementation
MGG_00138-UP-F	aagggaacaaaagctggtaccCGTTGAGCCTGCGGTTTTAT	Gene deletion
MGG_00138-Up-R	tcagttaacgtcgacaagcttGAAGGTGGCGGTCTGTTTGT	Gene deletion
MGG_00138-down-F	cgggaaccagttaacctgcagTGGCATTGGCGTTTGTTGAG	Gene deletion
MGG_00138-down-R	cgctctagaactagtggatccCAGGAGCATTATTGCGTGGG	Gene deletion
MGG_01426-UP-F	aagggaacaaaagctggtaccGCTGGAGCGGCTTTGTTTGG	Gene deletion
MGG_01426-UP-R	tcagttaacgtcgacaagcttTGGAGATGAGCGGCGACTGG	Gene deletion
MGG_01426-DW-F	cgggaaccagttaacctgcagCAAACGAGAAGAAGGGGAAG	Gene deletion
MGG_01426-DW-R	cgctctagaactagtggatccGCGCACTATGAAAGGAAGCT	Gene deletion
MGG_08095-UP-F	aagggaacaaaagctggtaccGAACAAAGTTGAAAAGAGCG	Gene deletion
MGG_08095-UP-R	tcagttaacgtcgacaagcttAAATCCTGGATAATCGAGCA	Gene deletion
MGG_08095-DW-F	cgggaaccagttaacctgcagTATAATTCATGAGGCCACCT	Gene deletion
MGG_08095-DW-R	cgctctagaactagtggatcccCTATTCTTCTCCCTTTTGCT	Gene deletion
MGG_02746-UP-F	aagggaacaaaagctggtaccGTAAGTAAGGTGTAGGAGCG	Gene deletion
MGG_02746-UP-R	tcagttaacgtcgacaagcttCGACTAATAAGAAAGCGGAG	Gene deletion
MGG_02746-DW-F	cgggaaccagttaacctgcagTGGGGAGAACTTTGTGTGGA	Gene deletion
MGG_02746-DW-R	cgctctagaactagtggatccTTGAGGGTCAGGGTTGAGGA	Gene deletion
pCB1532-MG02746- BamH1-F	cgctctagaactagtggatcccCCGTAGTCAATTGTGTCGC	Gene complementation
pCB1532-MG02746-EcoR1-R	gcccttgctcaccatgaattcTTTCTGCGTGTCGTCTAGAAGC	Gene complementation
MGG_03899-UP-F:	aagggaacaaaagctggtaccCAAATGAAGCAGCGGACAGC	Gene deletion
MGG_03899-UP-R	tcagttaacgtcgacaagcttACCATAGAAATTACCAGGAA	Gene deletion
MGG_03899-DW-F	cgggaaccagttaacctgcagGTTATATGGTGTTTTAGGAG	Gene deletion
MGG_03899-DW-R	cgctctagaactagtggatccGGAAGTTGTTGAATTTAGTG	Gene deletion
MGG_10426-UP-F	aagggaacaaaagctggtaccGAATAACAACCAACTCCTCC	Gene deletion
MGG_10426-UP-R	tcagttaacgtcgacaagcttCATAAAATCCGTTTCTCAGC	Gene deletion
MGG_10426-DW-F	cgggaaccagttaacctgcagGCTTTGCTCGGTGTTGATTT	Gene deletion
MGG_10426-DW-R	cgctctagaactagtggatcccCTTTGGTTGATGCCTCCTGT	Gene deletion
pCB1532-MGG_10426-BamH1-F	cgctctagaactagtggatccAACAGCCTACGACATCCCAAG	Gene complementation
pCB1532-MGG_10426-EcoR1-R	gcccttgctcaccatgaattcCTGCTCGATCGTCATTTGACT	Gene complementation
MGG_05099-UP-F	aagggaacaaaagctggtaccAATGTCTTCTCGTATTTCGG	Gene deletion
MGG_05099-UP-R:	tcagttaacgtcgacaagcttTGGTAGTCGTGTAGCTGTTT	Gene deletion
MGG_05099-DW-F	cgggaaccagttaacctgcagTCGGGCGTGTACTAGGGATA	Gene deletion

MGG_05099-DW-R	cgctctagaactagtggatccCCAACTTTGGAAAGTTTGGC	Gene deletion
MGG_05945-UP-F	aagggaacaaaagctggtaccGTTGGGGTTTTTGGTTGTTT	Gene deletion
MGG_05945-UP-R	tcagttaacgtcgacaagcttGGTTTGGCACTCTCGTCTTA	Gene deletion
MGG_05945-DW-F	cgggaaccagttaacctgcagCGCACCTGACCCGAAACAAC	Gene deletion
MGG_05945-DW-R	cgctctagaactagtggatccTCCTCATGCCGACAAATGAA	Gene deletion
MGG_05240-UP-F	aagggaacaaaagctggtaccTGCTGCTTTCAATCTTGTTC	Gene deletion
MGG_05240-UP-R	tcagttaacgtcgacaagcttGATGGGCGTGATGCTCCGTG	Gene deletion
MGG_05240-DW-F	cgggaaccagttaacctgcagCACATGAATCATCCCACACC	Gene deletion
MGG_05240-DW-R	cgctctagaactagtggatccCAAAGCAACAGTCACTACCG	Gene deletion
MGG_06120-UP-F	aagggaacaaaagctggtaccGGGCAGCCTGCTCCACGAGT	Gene deletion
MGG_06120-UP-R	tcagttaacgtcgacaagcttATGGGAAGATGGGCGATTTT	Gene deletion
MGG_06120-DW-F	cgggaaccagttaacctgcagGTCCGTGCGTGTCCGTCTCT	Gene deletion
MGG_06120-DW-R	cgctctagaactagtggatcccCGCGGTGCAGCTGATTTTTT	Gene deletion
MGG_01133-UP-F	aagggaacaaaagctggtaccAGTTCATCTTGTGCTTGGGG	Gene deletion
MGG_01133-UP-R	tcagttaacgtcgacaagcttCGTTGGTGTGTACCTTTTGG	Gene deletion
MGG_01133-DW-F	cgggaaccagttaacctgcagCACTTTTTTTATACTGCGCT	Gene deletion
MGG_01133-DW-R	cgctctagaactagtggatccATCTTTTACCTGTTACGACC	Gene deletion
pCB1532-MGG_01133-BamH1-F	cgctctagaactagtggatccGGAGAATAGCGGCTAGACCT	Gene complementation
pCB1532-MGG_01133-EcoR1-R	gcccttgctcaccatgaattcTCTCGATTTGCCCGAGTTAGG	Gene complementation
MGG_06434-UP-F	aagggaacaaaagctggtaccggaagcactttcgtctcctg	Gene deletion
MGG_06434-UP-R	tcagttaacgtcgacaagctttaaaggggttgctggatttg	Gene deletion
MGG_06434-DW-F	cgggaaccagttaacctgcagcgcaaacaaaacgagtctca	Gene deletion
MGG_06434-DW-R	cgctctagaactagtggatccgctgttgtgggtgttgaatg	Gene deletion
MGG_05748-UP-F	aagggaacaaaagctggtaccctcggggctaagtttgattg	Gene deletion
MGG_05748-UP-R	tcagttaacgtcgacaagcttactgcgcttgttccgaatag	Gene deletion
MGG_05748-DW-F	cgggaaccagttaacctgcagtggtgacgaatgtctgtggt	Gene deletion
MGG_05748-DW-R	cgctctagaactagtggatccggacatgtacggcaaggatt	Gene deletion
MGG_01130-UP-F	aagggaacaaaagctggtacctcacaccccagtccacacta	Gene deletion
MGG_01130-UP-R	tcagttaacgtcgacaagcttttctgcgcctgtttttgtaa	Gene deletion
MGG_01130-DW-F	cgggaaccagttaacctgcagccgcgatagatgatttggat	Gene deletion
MGG_01130-DW-R	cgctctagaactagtggatcctggagggaaatgaagtttgc	Gene deletion
MGG_08137-UP-F	aagggaacaaaagctggtaccaggagcagttcgagttgtgg	Gene deletion
MGG_08137-UP-R	tcagttaacgtcgacaagcttaaagcttgagaagcgaggaa	Gene deletion
MGG_08137-DW-F	cgggaaccagttaacctgcagggccggattttacaatgcta	Gene deletion
MGG_08137-DW-R	cgctctagaactagtggatcctggcgacaaaagacaaaaca	Gene deletion
MGG_14558-UP-F	aagggaacaaaagctggtaccATGTGCGTACCTATTGCAACCT	Gene deletion
MGG_14558-UP-R	tcagttaacgtcgacaagcttGGTACCGGTCACGATCATCATA	Gene deletion
MGG_14558-DW-F	cgggaaccagttaacctgcagAGGAAAGGAAAGTACTTGATGG	Gene deletion
MGG_14558-DW-R	cgctctagaactagtggatccAAGTCTTGCGGTAGTCGAGCTT	Gene deletion
pCB1532-MGG_14558-BamH1-F	cgctctagaactagtggatccACAGCCAACATCATGCAAGACA	Gene complementation
pCB1532-MGG_14558-EcoR1-R	gcccttgctcaccatgaattcTCGCCCGTATCGATCCCG	Gene complementation
MGG_00138-XbaI-F	tacccaagcatccaatctagaATGCTCAAGAAGAAAGGCGCC	Protein localization
MGG_00138-EcoRI-R	gcccttgctcaccatgaattcACCACCAATCCCAACAAATCG	Protein localization
MGG_01426-XbaI-F	tacccaagcatccaatctagaATGCCTGTCGTCAAAGGAGGG	Protein localization
MGG_01426-EcoRI-R	gcccttgctcaccatgaattcGTGGTACCCATTAGTAACCACAG	Protein localization
MGG_08985-XbaI-F	tacccaagcatccaatctagaATGACTTCACTCGACGTCCGC	Protein localization

MGG_08985-EcoRI-R	gcccttgctcaccatgaattcACGTTTCTGTCTCTTGCCCTTG	Protein localization
MGG_08137-XbaI-F	tacccaagcatccaatctagaATGGCCCCCGGCAAGGAC	Protein localization
MGG_08137-EcoRI-R	gcccttgctcaccatgaattcTGCTTCGCCTCCAACCTTG	Protein localization
MGG_03899-XbaI-F	tacccaagcatccaatctagaATGGCTGAGATGTCGCTAGGC	Protein localization
MGG_03899-EcoRI-R	gcccttgctcaccatgaattcCCCGGTTGCTTTGGCAAG	Protein localization
MGG_06434-XbaI-F	tacccaagcatccaatctagaATGAAGTGGATGCGGACAGACT	Protein localization
MGG_06434-EcoRI-R	gcccttgctcaccatgaattcTTCGGCAGGCCTTCCAGG	Protein localization
MGG_05099-XbaI-F	tacccaagcatccaatctagaATGGGTGTCATACGGAAAAAGACA	Protein localization
MGG_05099-EcoRI-R	gcccttgctcaccatgaattcAGCCTTGCCAACCCATCC	Protein localization
MGG_06898-XbaI-F	tacccaagcatccaatctagaATGACTCTACCCATTTCGCCAA	Protein localization
MGG_06898-EcoRI-R	gcccttgctcaccatgaattcGTTCATGATGGAGGCGATCG	Protein localization
MGG_05945-XbaI-F	tacccaagcatccaatctagaATGCCCAAAATCACGCGA	Protein localization
MGG_05945-EcoRI-R	gcccttgctcaccatgaattcGACGCCGTGGTGTCCAGA	Protein localization
MGG_05240-XbaI-F	tacccaagcatccaatctagaATGAGCAGCCACTCGGGG	Protein localization
MGG_05240-EcoRI-R	gcccttgctcaccatgaattcTAAGGGACTTCCAAGTGGATGTC	Protein localization
MGG_06120-XbaI-F	tacccaagcatccaatctagaATGGCATCAAGATGGAATCTTCG	Protein localization
MGG_06120-EcoRI-R	gcccttgctcaccatgaattcCAAGGGTAGGAGATCCTCAACTGC	Protein localization
MGG_01130-XbaI-F	tacccaagcatccaatctagaATGTCTCCGATGCACATGAGC	Protein localization
MGG_01130-EcoRI-R	gcccttgctcaccatgaattcTGCGCCAACCCTTTCCTC	Protein localization
MGG_05748-XbaI-F	tacccaagcatccaatctagaATGCTTCTCCCCTCTGCAGTC	Protein localization
MGG_05748-EcoRI-R	gcccttgctcaccatgaattcCCTGGACTTTGCTAGACGAGCT	Protein localization
MGG_01720-F	cttgaccgtctggcctttag	RT-qPCR
MGG_01720-R	tggtcacatcttgtgccatt	RT-qPCR
MGG_01012-F	ccaaagaggtcaaacccaaa	RT-qPCR
MGG_01012-R	ccttgcggtagaaagcagtc	RT-qPCR
MGG_00138-F	cagcgcaagactccacagta	RT-qPCR
MGG_00138-R	atgctcgtgattgagcctct	RT-qPCR
MGG_01426-F	gagagggagagctggaggat	RT-qPCR
MGG_01426-R	cgagtaagagccaaccaagc	RT-qPCR
MGG_08095-F	gtttcattccacgaccgact	RT-qPCR
MGG_08095-R	ttcgtaatacgctgctgctg	RT-qPCR
MGG_08137-F	acgtcaccaacgctttctct	RT-qPCR
MGG_08137-R	tcgtttacgacgatgctgag	RT-qPCR
MGG_02746-F	gcagctaccacttcgcctac	RT-qPCR
MGG_02746-R	gtgttccggctgagaatcat	RT-qPCR
MGG_03899-F	gccaagaacgggatatctga	RT-qPCR
MGG_03899-R	ctgctgccttgtccttatcc	RT-qPCR
MGG_10426-F	ggatgtcgcagtttgaggtt	RT-qPCR
MGG_10426-R	tcgcggaggtcttctaggta	RT-qPCR
MGG_06434-F	tgtttgaccctgagatgcag	RT-qPCR
MGG_06434-R	cagtgcgcgactcatagaaa	RT-qPCR
MGG_05099-F	tcttgatcagaccccagacc	RT-qPCR
MGG_05099-R	tccttgagcaactgctcctt	RT-qPCR
MGG_06898-F	gacacctgcctccaattgtt	RT-qPCR
MGG_06898-R	ctcgtgatgcgctttgtcta	RT-qPCR

MGG_05945-F	actcgagcgcagtttacgat	RT-qPCR
MGG_05945-R	gcactgatacctgcagacga	RT-qPCR
MGG_05240-F	caaagacccagaggaccaaa	RT-qPCR
MGG_05240-R	gacctcccagggaagaactc	RT-qPCR
MGG_06120-F	gacggttgagactggtggtt	RT-qPCR
MGG_06120-R	aagtctgcgctccacttcat	RT-qPCR
MGG_01130-F	ccatgaatctcgttccgtct	RT-qPCR
MGG_01130-R	ctgttggctgacatgatgct	RT-qPCR
MGG_01133-F	gctgaagagcacatgctgaa	RT-qPCR
MGG_01133-R	gcttcttcacactcccttcg	RT-qPCR
MGG_05748-F	aacaacaacaacggccaact	RT-qPCR
MGG_05748-R	tttgtggtgcttttgctgtc	RT-qPCR
MGG_14558-F	tcgatagagcatcccgtacc	RT-qPCR
MGG_14558-R	atctggtgaattgggtctcg	RT-qPCR
MGG_00138-TZ-F	ACAGTGGCACGAGAGGTGGT	Southern blot probe
MGG_00138-TZ-R	CGCATGTAGTCGAAGAGATAGAT	Southern blot probe
MGG_01012-TZ-F	gactttcgggacaagatgga	Southern blot probe
MGG_01012-TZ-R	acacccatcgcgaatagaac	Southern blot probe
MG01130-TZ-F	tctgcacgttgcgtaggtag	Southern blot probe
MG01130-TZ-R	cgtcctcagggttttgacat	Southern blot probe
MGG_01133-TZ-F	tctgcacgttgcgtaggtag	Southern blot probe
MGG_01133-TZ-R	cgtcctcagggttttgacat	Southern blot probe
MGG_01426-TZ-F	cgcgtttcttcaaagactcc	Southern blot probe
MGG_01426-TZ-R	aaagtggggacaaacgtcac	Southern blot probe
MGG_01720-TZ-F	TGTTGGAAAGAGCGGGAGCA	Southern blot probe
MGG_01720-TZ-R	AAGCGTGGATTGGCGAGATA	Southern blot probe
MGG_02746-TZ-F	GCCAAGCGGGACCTTACAAT	Southern blot probe
MGG_02746-TZ-R	GGAGGAGCCATCACGAGAATA	Southern blot probe
MGG_05099-TZ-F	AAGTGGGCTGGATGTTGTTT	Southern blot probe
MGG_05099-TZ-R	CTTGGTAGTCGTGTAGCTGTTTAA	Southern blot probe
MGG_05240-TZ-F	gcagcatgtgtcgatgattt	Southern blot probe
MGG_05240-TZ-R	actgtttacgaggcgaagga	Southern blot probe
MGG_05945-TZ-F	ctcttggatgaccacccact	Southern blot probe
MGG_05945-TZ-R	caaatgaaaggggtttcacg	Southern blot probe
MGG_08095-TZ-F	GAGTAGAACAAAGTTGAAAAGAGCG	Southern blot probe
MGG_08095-TZ-R	CTGGGGAGTAATTGGGAGGA	Southern blot probe
MGG_10426-TZ-F	gacgatgacgacgaagatca	Southern blot probe
MGG_10426-TZ-R	gtctttgccaagaaggcaag	Southern blot probe
MGG_14558-TZ-F	TGCGTGTTTAGAGCTTGTGC	Southern blot probe
MGG_14558-TZ-R	ATTGGCGTGCCTTTTGGT	Southern blot probe

Table S2

	Myb	Deleted	MY	Con	8hpi	24hpi	48hpi	72hpi	96hpi	Profile			
MGG_01720	Myb17	O	0.29377	2.42739	0.87019	0.43711	2.6996	1.5613	1.12981		48-96HPI and MY		
MGG_00138	Myb16	X	0.26869	3.17626	0.40819	0.69448	4.62889	1.88862	1.59181				
MGG_15357	Myb12	O	0.11866	4.32665	0.50869	0.39091	1.63571	1.67785	1.49131				
MGG_10426	Myb2	X	0.13445	2.89151	0.53407	0.29494	2.832	0.87167	1.46593				
MGG_01012	Myb15	X	0.15935	2.26624	0.7686	0.41188	1.68994	1.141	1.2314				
MGG_01426	Myb4	X	0.05159	1.40114	0.1297	0.21713	0.86051	0.74395	1.8703		Conidia late (formation)		
MGG_01133	Myb5	X	0.10831	5.86972	0.12101	0.09898	0.65065	0.8766	1.87899				
MGG_01130	Myb6	X	0.08542	0.17164	0.18395	0.54365	1.80768	0.4777	1.81605				
MGG_05748	Myb10	X	0.14046	6.18289	0.67901	0.63356	0.66202	0.41418	1.32099				
MGG_05240	Myb9	X	0.03941	0.3715	0.82057	1.73475	1.53485	1.02202	1.17943		24HPI		
MGG_06120	Myb19	O	0.23444	0.42749	0.66767	1.90164	0.62877	0.72898	1.33233				
MGG_08095	Myb9	X	0.36388	1.46227	1.18499	0.7764	0.5427	0.47904	0.81501		Little regulation		
MGG_05099	Myb12	X	0.20749	1.79146	1.05538	0.33089	0.2874	0.60759	0.94462				
MGG_03899	Myb14	X	0.08897	1.09643	1.66564	0.22732	0.33903	0.14622	0.33436		8HPI		
MGG_06898	Myb1	X	0.00636	0.37845	1.96182	0.83833	0.0172	0.02004	0.03818				
MGG_02746	Myb7	O	0.19945	2.77815	1.59925	0.27626	0.07351	0.3101	0.40075				
MGG_08137	Myb3	X	0.08723	0.8337	1.36378	0.8053	0.23667	0.5252	0.63622				
MGG_05945	Myb8	X	0.02566	0.07209	1.07608	1.00636	0.14351	0.52577	0.92392				
MGG_14558	Myb13	X	0.10274	2.97662	1.23138	0.68951	0.91194	0.45073	0.76862				

Table S3

Sequences producing significant alignments with more than 70 percent cover:

Sequences	Description	Scientific Name	Max Score	Total Score	Query Cover	E value	Per. Ident	Acc. Len	Accession
Select seq ref|XP_003709785.1|	uncharacterized protein MGG_14558 [Pyricularia oryzae 70-15]	Pyricularia oryzae 70-15	4526	4526	100%	0	100.00%	2305	XP_003709785.1
Select seq gb|ELQ36651.1|	hypothetical protein OOU_Y34scaffold00649g34 [Pyricularia oryzae Y34]	Pyricularia oryzae Y34	4510	4510	100%	0	99.91%	2615	ELQ36651.1
Select seq gb|QBZ54440.1|	hypothetical protein PoMZ_10140 [Pyricularia oryzae]	Pyricularia oryzae	4444	4444	100%	0	98.11%	2632	QBZ54440.1
Select seq gb|ELQ68318.1|	hypothetical protein OOW_P131scaffold00255g20 [Pyricularia oryzae P131]	Pyricularia oryzae P131	4404	4404	100%	0	97.87%	2571	ELQ68318.1
Select seq gb|ROW02559.1|	hypothetical protein VPNG_07863 [Cytospora leucostoma]	Cytospora leucostoma	555	681	90%	7.00E-158	37.34%	2285	ROW02559.1
Select seq gb|KUI62100.1|	hypothetical protein VP1G_09221 [Valsa mali var. pyri]	Valsa mali var. pyri	530	659	86%	2.00E-149	36.63%	2284	KUI62100.1
Select seq gb|OIW27663.1|	hypothetical protein CONLIGDRAFT_682689 [Coniochaeta ligniaria NRRL 30616]	Coniochaeta ligniaria NRRL 30616	614	723	82%	5.00E-178	39.22%	2253	OIW27663.1
Select seq gb|KAB5585523.1|	hypothetical protein GE09DRAFT_29357 [Coniochaeta sp. 2T2.1]	Coniochaeta sp. 2T2.1	579	690	78%	4.00E-166	38.69%	2211	KAB5585523.1
Select seq gb|KAA8631205.1|	hypothetical protein SMACR_04153 [Sordaria macrospora]	Sordaria macrospora	506	782	78%	3.00E-141	43.08%	2610	KAA8631205.1
Select seq gb|KAH7635984.1|	hypothetical protein B0T09DRAFT_31245 [Sordaria sp. MPI-SDFR-AT-0083]	Sordaria sp. MPI-SDFR-AT-0083	506	781	78%	5.00E-141	42.98%	2687	KAH7635984.1
Select seq gb|TRX97365.1|	hypothetical protein FHL15_001643 [Xylaria flabelliformis]	Xylaria flabelliformis	535	609	77%	4.00E-152	36.34%	2024	TRX97365.1
Select seq gb|RYP84680.1|	hypothetical protein DL769_001114 [Monosporascus sp. CRB-8-3]	Monosporascus sp. CRB-8-3	604	664	76%	7.00E-176	37.46%	2020	RYP84680.1
Select seq gb|RYP88518.1|	hypothetical protein DL770_004599 [Monosporascus sp. CRB-9-2]	Monosporascus sp. CRB-9-2	598	652	76%	2.00E-173	36.53%	2035	RYP88518.1
Select seq ref|XP_030990550.1|	uncharacterized protein E0L32_009657 [Phialemoniopsis curvata]	Phialemoniopsis curvata	531	934	75%	5.00E-151	42.68%	2017	XP_030990550.1
Select seq ref|XP_024511445.1|	uncharacterized protein SMAC_04153 [Sordaria macrospora k-hell]	Sordaria macrospora k-hell	508	780	73%	1.00E-141	43.08%	2675	XP_024511445.1
Select seq gb|KAH6848250.1|	hypothetical protein B0I37DRAFT_159719 [Chaetomium sp. MPI-CAGE-AT-0009]	Chaetomium sp. MPI-CAGE-AT-0009	509	768	72%	2.00E-143	40.27%	2000	KAH6848250.1
Select seq gb|RYP04937.1|	hypothetical protein DL764_004149 [Monosporascus ibericus]	Monosporascus ibericus	484	692	71%	3.00E-135	40.63%	2014	RYP04937.1